Article

Optimal Network Reconfiguration in Active Distribution Networks with Soft Open Points and Distributed Generation

Ibrahim M. Diaaeldin [1], Shady H. E. Abdel Aleem[2,*], Ahmed El-Rafei [3], Almoataz Y. Abdelaziz [4] and Ahmed F. Zobaa [5,*]

[1] Engineering Physics and Mathematics Department, Ain Shams University, Cairo, Egypt; ibrahimmohamed@eng.asu.edu.eg; ibrahimmohamed@ieee.org
[2] Mathematical, Physical and Engineering Sciences Department, 15th of May Higher Institute of Engineering, Cairo, Egypt; engyshady@ieee.org; shossam@theiet.org
[3] Engineering Physics and Mathematics Department, Ain Shams University, Cairo, Egypt; ahmed.elrafei@eng.asu.edu.eg
[4] Electric Power and Machines Department, Ain Shams University, Cairo, Egypt; almoataz_abdelaziz@eng.asu.edu.eg; almoataz.abdelaziz@fue.edu.eg; almoataz.abdelaziz@ieee.org
[5] Electronic and Computer Engineering Department, Brunel University London, Uxbridge UB8 3PH, U.K.; azobaa@ieee.org
* Correspondence: engyshady@ieee.org; Tel.: +2-01227567489

Abstract: In this paper, a recent meta-heuristic optimization algorithm called the discrete-continuous hyper-spherical search algorithm is used to solve the mixed-integer nonlinear problem of soft open points (SOPs) and renewable distributed generators allocation along with new network reconfiguration methodology under different loading conditions to minimize the total power loss in balanced distribution systems. Multi-scenario studies, which aim to improve the investigation of the overall performance of the strategies, are conducted on IEEE 33-node and 83-node balanced distribution systems. The contributions of SOP losses to the total active losses, as well as the effect of increasing the number of SOPs connected to the system, are investigated to determine the real benefits gained from their allocation. The results obtained validate, with proper justifications, the effectiveness of allocating both SOPs and renewable distributed generators with the proposed network reconfiguration methodology to provide the best operation of distribution networks with minimum losses and enhanced power quality performance. It was also shown that SOPs successfully assist the growing integration plans of the renewable distributed generators units and can address issues related to voltage violations and network losses efficiently.

Keywords: Distributed generator, load balancing, network reconfiguration, optimization, power loss minimization, soft open points.

Abbreviations:

ADN	Active distribution network
B2B VSC	Back-to-back voltage source converter
BLP	Bi-level programming
CB	Capacitor bank
D-HSS	Discrete hyper-spherical search algorithm
DC-HSS	Discrete-continuous HSS algorithm
DG	Distributed generation
EA	Evolutionary algorithm
ESS	Energy storage system
HC	Hosting capacity
HSS	Hyper-spherical search algorithm

HSA	Harmony search algorithm
MHM	Modified honeybee mating
MINLP	Mixed-integer nonlinear programming
MISOCP	Mixed-integer second-order cone programming
NR	Network reconfiguration
PF	Power factor
PQ	Power quality
PSO	Particle swarm optimization
SOP	Soft open point
SOCP	Second-order cone programming
SC	Sphere-center
VSC	Voltage source converter
VD	Voltage deviation
GA	Genetic algorithm

36 **Nomenclature:**

A_{loss}^{SOP}	Loss coefficient of VSCs
$AVDI$	Aggregate voltage deviation index
AP	The assigning probability
D_{SC}	Normalized dominance for each SC
$DSOF$	Difference of set objective functions for each set of particles and their sphere-center
f_{SC}	Objective function value for each SC
$f_{particles\ of\ SC}$	Objective function value for each particle assigned to a SC
I_b	line current flowing in line b
I_b^{rated}	Rated line current flowing in line b
LBI_b	Load balancing index of line b
LBI_{tot}	Total load balancing index
Max_{iter}	Maximum number of iterations
M	Incidence matrix
N_{br}	Number of lines existing in the distribution network
N_n	Number of nodes existing in the distribution network
N_f	Number of feeders
N_{DG}	Number of distributed generators
N_{SOP}	Number of allocated SOPs
N_{pop}	Population size
N_{SC}	Number of sphere-centers
N_{newpar}	Number of new generated particles
N	Number of decision variables
OFD	Objective function difference
Pr_{angle}	Probability of changing particle's angle
P_i, Q_i	Active and reactive power injected at the i^{th} node
P_i^L, Q_i^L	Active and reactive power of the connected load to the i^{th} node
P_i^{DG}, Q_i^{DG}	Active and reactive DG power injected at the i^{th} node
P_I^{SOP}, Q_I^{SOP}	SOP active and reactive power injected to the I^{th} feeder
$P_I^{SOP-loss}$	Internal power loss of the converter connected to the I^{th} feeder
P_{loss}^{tot}	Total active power losses
$P^{SOP-loss}$	SOP's internal power losses

Preprints (www.preprints.org) | NOT PEER-REVIEWED | Posted: 30 September 2019 doi:10.20944/preprints201909.0339.v1

Peer-reviewed version available at Energies 2019, 12, 4172; doi:10.3390/en12214172

$Q_I^{SOP-min}$, $Q_I^{SOP-max}$	Minimum and maximum SOP reactive injected to the I^{th} feeder
$r_{i,i+1}$, $x_{i,i+1}$	Line resistance and reactance between nodes i and $i+1$
r, θ	Distance and angle between the particle and the sphere-center
r_{min}, r_{max}	Minimum and maximum radius of the sphere-center for continuous HSS
$r_{d,min}$, $r_{d,max}$	Minimum and maximum radius of the sphere-center for discrete HSS
S_I^{SOP}	Maximum capacity limit of the planned SOP
S^{DG}	Maximum capacity limit of the installed DGs
SOF	Set objective function
μ	Binary variable set to 1 if the SOP loss is considered and to 0 if the SOP loss is not considered.
$\lvert V_i \rvert$	Magnitude of the voltage at the i^{th} node
V_{min}, V_{max}	Minimum and maximum voltage limits
X_{rand}	Random binary vector
X_{temp}	Temporary binary vector
D_{temp}	A vector equal to the difference between the temporary and random vectors
X_{check}	Reconfiguration checking vector
X_{best}^{rec}	Best reconfiguration vector
x_i	A vector of decision variables
$X_{i_{min}}$, $X_{i_{\max}}$	Minimum and maximum values of continuous decision variables
$X_{id,min}$, $X_{id,max}$	Minimum and maximum values of discrete decision variables
β_{min}	Minimum lagging power factor

1. Introduction

The high penetration of distributed generation (DG) units has resulted in new challenges for the planning and operation of power distribution systems, such as power loss increase, harmonic distortion aggregation, equipment overloads, and voltage quality problems. Thus, there is significant room for improvement and new perceptions to face these challenges are needed to cope with future advances in order to realize resilient electrical distribution systems with high renewables penetration and guarantee reliable and efficient network performance. In this regard, transmission and distribution network operators are facing a great challenge to identify the sources of network losses, utilize appropriate solutions to ensure reduced losses, operational costs and emissions, while keeping future energy losses as low as possible through proper planning of distribution systems with low carbon technologies [1], [2].

Traditionally, power loss can be minimized via several methods such as using power quality (PQ) devices to enhance the PQ performance of a system by limiting inefficiencies in the way power is transferred and reducing harmonic distortion, which result in increased loss in distribution networks [3]; reducing network imbalance, as an unbalanced power system will have higher currents in one or more phases compared to balanced power systems [4]; improving the power factor (PF) where low PF circuits suffer from a significant increase in the current at the same power delivered [5]; configuring power system networks to provide a flexible framework to transfer electrical loads between feeders that result in minimized loss and improved balancing of loads [6]; upgrading networks to higher voltage levels while expanding reinforcement plans to guarantee significant loss savings [7], [8] considering enhanced demand response programs to reschedule energy usage and improve the reliability and efficiency of electrical networks and consequently reduce losses [9]; and allocating DG units and power electronic devices in the distribution network [10] to control power delivery between interlinked feeders and reduce power loss efficiently. However, it is prudent to

Preprints (www.preprints.org) | NOT PEER-REVIEWED | Posted: 30 September 2019 doi:10.20944/preprints201909.0339.v1

Peer-reviewed version available at Energies 2019, 12, 4172; doi:10.3390/en12214172

ensure that DGs or electronic devices are optimally sized and connected to suitable locations in power systems to take full advantage of their positive benefits [1], [6].

Power systems are electrically separated via open points (switches). These open points are strategically positioned to balance loads and hence reduce losses. Hence, network reconfiguration (NR) can be performed by changing the state of sectionalized (closed) and tie (open) switches, considering the need not to lose the radiality of the system. In the literature, NR has been applied in different works to minimize network losses, improve the voltage profile, balance loads between two or more feeders, and reduce the need for network reinforcement, while considering the influence and increase of penetration of the DG units [6]. Also, the NR problem can be solved while taking into account the optimal placement of shunt capacitors [11], harmonic filters [12] and power electronic devices [13] to control the flow of either reactive and active powers or both between the feeders they are connected to, because the extra power conditioners may be beneficial in some cases to enhance the operational flexibility of the existing configurations, leading to more cumulative benefits of reduced losses.

In this regard, soft open points (SOPs) are power electronic devices that can be placed instead of normally open/closed points to provide a fast response, frequent actions and enhanced control scheme for power flow between adjacent feeders they are connected to. In the near past, the optimal operation of SOPs was investigated in balanced and unbalanced active distribution networks [14], [15]. Several design strategies are manipulated for their optimal operation, such as the minimization of energy loss [15] or annual expense [16] in a system, loads balancing [17], voltage profile enhancement [18], and increasing the renewables hosting capacity [19] in distribution systems. Various single-objective and multi-objective optimization techniques were used to solve these optimization problems. Table 1 presents an overview of research works that have addressed SOPs design and operation [15]–[34].

Some researchers such as Xiao et al. [34] did not consider the active power loss of the SOP although there is active power loss in the SOP itself. However, they assumed that the active power loss of the SOP is relatively small when compared to the entire distribution system losses. On the other hand, the impact of the internal active losses of SOPs was presented in many research works, but the influence of SOPs' power loss on the system performance, its share in the total active power loss, and the effect of increasing the number of SOPs connected to the system are not investigated in these works. Also, throughout the literature, one can see that most of the studies concerned with NR and SOPs assume a fixed number and location of the SOP, which might not result in optimal operational performance, in addition to permitting reverse power flow in the systems considered in these studies. Moreover, optimizing the NR, DGs allocation and SOPs placement strategies separately has some drawbacks, such as the lack of collaboration between strategies, which may lead to sub-optimal overall performance and an inability to model the correlation between the benefits of each strategy. To redress these gaps, in this study, we are motivated to allocate SOPs and DGs simultaneously with and without NR and investigate the contribution of SOP losses to the total active losses, as well as the effect of increasing the number of SOPs connected to the studied systems under different loading conditions to determine the real benefits gained from each strategy. In addition, an analytical NR approach is proposed to obtain radial configurations in an efficient manner without the possibility of getting trapped in local minima. Further, multi-scenario studies, which aim to improve the investigation of the overall performance of the strategies, are conducted on an IEEE 33-node balanced benchmark distribution system and an 83-node balanced distribution system from a power company in Taiwan.

Preprints (www.preprints.org) | NOT PEER-REVIEWED | Posted: 30 September 2019 doi:10.20944/preprints201909.0339.v1

Peer-reviewed version available at *Energies* **2019**, *12*, 4172; doi:10.3390/en12214172

Table 1. Overview of research works addressing SOPs design and operation

Ref.	Scope*	Year	Objective	Optimization technique	SOP	NR	DG	CB	ESS	OLTC	System	Remarks
[15]	PS	2016	Loss minimization and LBI	Improved Powell's Direct Set	√	√	√	×	×	×	33-node	A study was conducted to compare NR and SOP. A new methodology was proposed to combine NR and SOP.
[19]	PS	2017	HC maximization	Strengthened SOCP	√	×	√	×	×	×	33-node	A strengthened SOCP was proposed to verify the exactness of the optimality gap to maximize the HC of the system.
[20]	PE	2016	Studying the operation of SOPs	×	√	×	×	×	×	×	MV distribution network	The operating principles for the placement of SOPs under normal, fault and post-fault conditions were discussed.
[21]	PE	2018	Fault detection	×	√	×	×	×	×	×	×	A new index was proposed to detect faults based on local measurements of the symmetrical voltages.
[24]	PS	2017	Power loss minimization	PSO	√	×	√	×	×	×	Anglesey network	The main aim was to convert an existing double 33 kV AC circuit to DC operation to increase the HC of the network.
[22]	PS	2016	Annual costs minimization	MISOCP	√	×	√	×	×	×	33-node	A mixed-integer SOCP was proposed to minimize annual expenses, which comprise the investment cost of SOPs, operation cost of SOPs and power loss expenses.
[23]	PS	2017	DGs penetration maximization	Ant colony	√	√	√	×	×	×	33-node	Different scenarios were conducted to maximize DGs penetration.
[16]	PS	2017	Minimization of annual cost and power loss	BLP	√	×	√	√	×	×	33-node	Bi-level programming was used to find the optimal allocation of DGs, CBs and a SOP where the annual costs and power losses were considered as the problem levels.
[25]	PS	2019	Combined minimization of total power loss and VD	MISOCP	√	×	√	×	×	×	69-node and 123-node	A decentralization method was proposed to reduce the dependency on a massive communication and computation burden.
[26]	PS	2018	Power loss minimization	Sequential optimization	√	×	√	×	√	×	33-node	A new approach was introduced to gain the benefits of both SOPs and ESS. A sequential optimization model was used to minimize network losses, converter losses and ESS losses.

Peer-reviewed version available at Energies 2019, 12, 4172; doi:10.3390/en12214172

Ref.	Scope*	Year	Objective	Optimization technique	SOP	NR	DG	CB	ESS	OLTC	System	Remarks
[27]	PS	2016	HC maximization	×	√	×	√	×	×	×	Generic system	HC maximization gained from insertion of a SOP between two distinct 33 kV networks were presented.
[28]	PS	2016	Power loss minimization	MISOCP	√	√	√	×	×	×	33-node	A new methodology to allocate a SOP along with NR simultaneously considering the cost of switching actions and SOP losses was presented.
[29]	PS	2017	Minimization of ESS costs	MISOCP	√	√	√	×	√	√	33-node	Optimally sited and sized ESSs in an ADN that includes SOP and DGs smart inverters were presented.
[30]	PS	2017	LBI and power loss minimization	SOCP	√	×	√	×	×	×	33-node	Installation of a multi-terminal SOP using an enhanced SOCP-based method was proposed.
[31]	PS	2018	Restored loads maximization	Primal-dual interior-point	√	×	√	×	√	×	33-node and 123-node	SOP islanding partitioning of ADNs with DGs, loads and ESSs time series characteristics was presented.
[32]	PS	2017	Operation cost and VD minimization	MISOCP	√	×	√	√	√	√	33-node and 123-node	Optimal coordination between OLTC, CBs and SOP using a time-series model was presented.
[17]	PE	2016	VD, LBI and energy loss minimization	Interior-point	√	×	√	×	×	×	MV distribution network	A Jacobian matrix-based sensitivity method was proposed to operate a SOP under various conditions.
[18]	PS	2017	Power loss, LBI and VD minimization	MOPSO and Taxicab	√	√	√	×	×	×	69-node	Optimal allocation of SOP with NR at various DGs penetrations was presented.
[33]	PS	2017	Annual expenses minimization	MISOCP	√	√	√	×	×	×	33-node and 83-node	A new concept was presented to install SOPs in normally closed lines as well as normally open lines.
[34]	PS	2018	Voltage imbalance	Improved differential evolution algorithm	√	×	√	×	×	×	Hybrid distribution system	Optimal allocation of SOPs to improve 3-phase imbalance with DGs and loads uncertainties were proposed using an improved differential evolution algorithm.

108 *PS denotes a power system perspective and PE denotes a power electronics perspective

Preprints (www.preprints.org) | NOT PEER-REVIEWED | Posted: 30 September 2019 doi:10.20944/preprints201909.0339.v1

Peer-reviewed version available at Energies 2019, 12, 4172; doi:10.3390/en12214172

The multi-scenario studies investigated in this work are: 1) NR as a stand-alone strategy, 2) DGs allocation as a stand-alone strategy, 3) simultaneous NR and DGs allocation, 4) SOPs allocation without NR, 5) SOPs allocation after NR is performed, 6) simultaneous SOPs allocation and NR, 7) simultaneous SOPs and DGs allocation without NR, 8) simultaneous SOPs and DGs allocation after NR is performed, and 9) simultaneous NR and SOPs and DGs allocation.

A recent meta-heuristic optimization algorithm called the discrete-continuous hyper-spherical search (DC-HSS) algorithm is used to solve the mixed-integer nonlinear problem (MINLP) of SOPs and DGs allocation along with NR to minimize power loss in the distribution systems. The DC-HSS has the advantages of fast convergence to the optimal/near-optimal solutions [35], [36].

The contribution of this work is twofold. First, we propose a new NR methodology to obtain the possible radial configurations from random configurations to minimize power loss in two distribution systems, taking into account different strategies for DGs, SOPs, and NR while considering multi-scenarios to improve the investigation of the overall performance of the strategies, and in turn their priorities. Second, the contribution of SOP losses to the total active losses as well as the effect of increasing the number of SOPs connected to the system are investigated under different loading conditions to determine the real benefits gained from SOPs and DGs allocation with network reconfiguration to provide the best operation of distribution networks with minimum losses and enhanced power quality performance. It was clear from the results obtained that placing SOPs and DGs into a distribution system creates a hybrid configuration that merges the benefits offered by radial and meshed distribution systems and mitigates drawbacks related to losses, PQ, and voltage violations, while offering far more efficient and optimal network operation.

The rest of the paper is organized as follows: Section II presents the problem statement, proposed NR methodology, modeling of SOPs and DGs, and PQ indices that evaluate the system performance. Further, Section III presents the problem formulation and the search algorithm used to solve the mixed-integer nonlinear problem. Section IV presents the results and discusses them, and Section V presents the conclusions and limitations of our study as well as a preview of future works.

2. Problem Statement

The NR, SOPs and DGs modeling, and PQ performance indices, namely the load balancing index (*LBI*), and aggregate voltage deviation index (*AVDI*), are presented and discussed. Hence, the formulation of the load flow calculations, the objective function to minimize the network active power loss, the constraint conditions of voltage, current, SOP capacity, active and reactive powers, and the DC-HSS algorithm proposed to solve the formulated MINLP problem are presented.

2.1. Proposed Network Reconfiguration

Distribution systems have sectionalizing switches (normally closed switches) that connect line sections and tie switches (normally open switches) that connect two primary feeders, two substation buses, or loop-type laterals. Each line is assumed a sectionalized line with a normally closed sectionalized switch in the line. Also, each normally open tie switch is assumed to be in each tie line. Thus, NR is the change that occurs in the status of tie and sectionalized switches to reconnect distribution feeders to form a new radial structure for a certain operation goal without violating the condition of having a radial structure. In this study, the procedure of NR to generate possible radial configurations in a fast and efficient manner is implemented analytically and is clarified as follows:

Step 1: A binary vector $X_{rand}^{(0)} = [1\ 0\ 0\ 1\ 1 \dots 1]_{1\times N_{br}}$ is initialized with random binary values, in which its length is equal to the number of lines (N_{br}) with its sectionalized and tie switches. The sectionalized switches are denoted "1" and the tie switches are denoted "0".

Step 2: The best reconfiguration vector of the system (X_{best}^{rec}), which represents the best vector that meets the radiality requirements (described in Step 6) and achieves the desired goal, is initialized with the base configuration of the system.

Step 3: A temporary vector $X_{temp}^{(0)}$ that is equal to X_{best}^{rec} is created. At that point, each element in $X_{temp}^{(0)}$ is compared with the corresponding element in $X_{rand}^{(0)}$ to create a new vector $D_{temp}^{(0)}$, in which

Preprints (www.preprints.org) | NOT PEER-REVIEWED | Posted: 30 September 2019 doi:10.20944/preprints201909.0339.v1

Peer-reviewed version available at *Energies* **2019**, *12*, 4172; doi:10.3390/en12214172

$D_{temp}^{(0)} = X_{temp}^{(0)} - X_{rand}^{(0)}$. Further, $\forall\, b \in N_{br}$, if $D_{temp}^{(0)}(b) = 1$, it means that this bth line is changed to a tie line in the random vector; also if $D_{temp}^{(0)}(b) = -1$, it means that the bth line is changed to a sectionalized line in the random vector. Otherwise, if $D_{temp}^{(0)}(b) = 0$, this indicates that no change has occurred.

Step 4: Starting from the first element in $D_{temp}^{(0)}$, if $D_{temp}^{(0)}(b) = 1$ and $D_{temp}^{(0)}(j) = -1$, where j denotes a random line selected from the remaining lines in the system with the condition that $b \neq j$, a vector $X_{check}^{(0)}$ is generated so that $X_{check}^{(0)}$ is equal to $X_{temp}^{(0)}$ subjected to $X_{check}^{(0)}(b) = 0$ and $X_{check}^{(0)}(j) = 1$. The vector $X_{check}^{(0)}$ is then checked for radiality described in Step 6. If it is found to be radial, then b is updated so that $b = b + 1$, and the vector $X_{temp}^{(1)}$ is generated equal to $X_{best}^{rec\,(1)}$. It should be mentioned that a set of $X_{check}^{(0)}$ vectors may be generated as soon as b is smaller than or equal to N_{br}, and the vectors found to be radial in this set are evaluated based on their fitness value to give the best X_{best}^{rec}.

Step 5: The steps will terminate when we achieve a very small distance among serial solutions by evaluation of the objective function.

Step 6: The procedure of radiality check is done as follows:

- Build an incidence matrix M where its rows and columns represent the lines and nodes of the distribution network, respectively. The nodes of each line are denoted "1" in M, and the rest of the elements in the row are denoted "0".
- Elements in the rows of each tie line are set to "0". Then, we create a vector S, in which its length is equal to the number of nodes, and each element e in S is equal to the sum of its corresponding e^{th} column in M. If an element in S is equal to "1", it means that this element represents an end node. Further, the row that corresponds to this end node in M is set to "0".
- Recalculate S and repeat the former process as soon as an element in S is equal to 1. At that point, calculate the sum of all the elements in M. If the sum is equal to zero, this means that the configuration is radial, otherwise, it is not radial.

An illustrative example for a 19-node system is given in Table 2 to clarify the proposed reconfiguration procedure, in which the lines changed to ties are shaded blue, and the lines changed to sectionalized are shaded yellow. Fig. 1(a) shows the initial configuration of the 19-node system. Figs. 1(b) and 1(c) show two possible attempts to obtain a new configuration of the system in the first two generations of the reconfiguration procedure. From that, it can be noted that the proposed algorithm can produce a series of radial configurations and modify the obtained non-radial configurations to be radial.

Table 2. Proposed NR Procedure

Line	1	2	3	4	5	6	7	8	9	10	11	12	13	14	15	16	17	18	19	20	Radiality
First generation																					
$X_{best}^{rec\,(0)}$	1	1	1	1	1	1	1	1	1	1	1	1	1	1	1	1	1	1	0	0	Yes
$X_{temp}^{(0)}$	1	1	1	1	1	1	1	1	1	1	1	1	1	1	1	1	1	1	0	0	Yes
$X_{rand}^{(0)}$	1	0	1	0	0	1	1	0	1	1	1	0	0	1	0	1	1	0	1	0	NA*
$D_{temp}^{(0)}$	0	1	0	1	1	0	0	1	0	0	0	1	0	0	1	0	0	1	-1	0	NA
$X_{check}^{(0)}$	1	0	1	1	1	1	1	1	1	1	1	1	1	1	1	1	1	1	1	0	Yes
Second generation																					
$X_{best}^{rec\,(1)}$	1	0	1	1	1	1	1	1	1	1	1	1	1	1	1	1	1	1	1	0	Yes
$X_{temp}^{(1)}$	1	0	1	1	1	1	1	1	1	1	1	1	1	1	1	1	1	1	1	0	Yes
$X_{rand}^{(1)}$	1	0	0	1	0	1	1	0	1	1	1	0	0	1	0	1	1	0	1	1	NA
$D_{temp}^{(1)}$	0	0	1	0	1	0	0	1	0	0	0	1	1	0	1	0	0	1	0	-1	NA
$X_{check}^{(1)}$	1	0	0	0	1	1	1	1	1	1	1	1	1	1	1	1	1	1	1	1	No
Third generation																					
$X_{best}^{rec\,(2)}$	1	0	1	1	1	1	1	1	1	1	1	1	1	1	1	1	1	1	1	0	Yes

*NA: not applicable

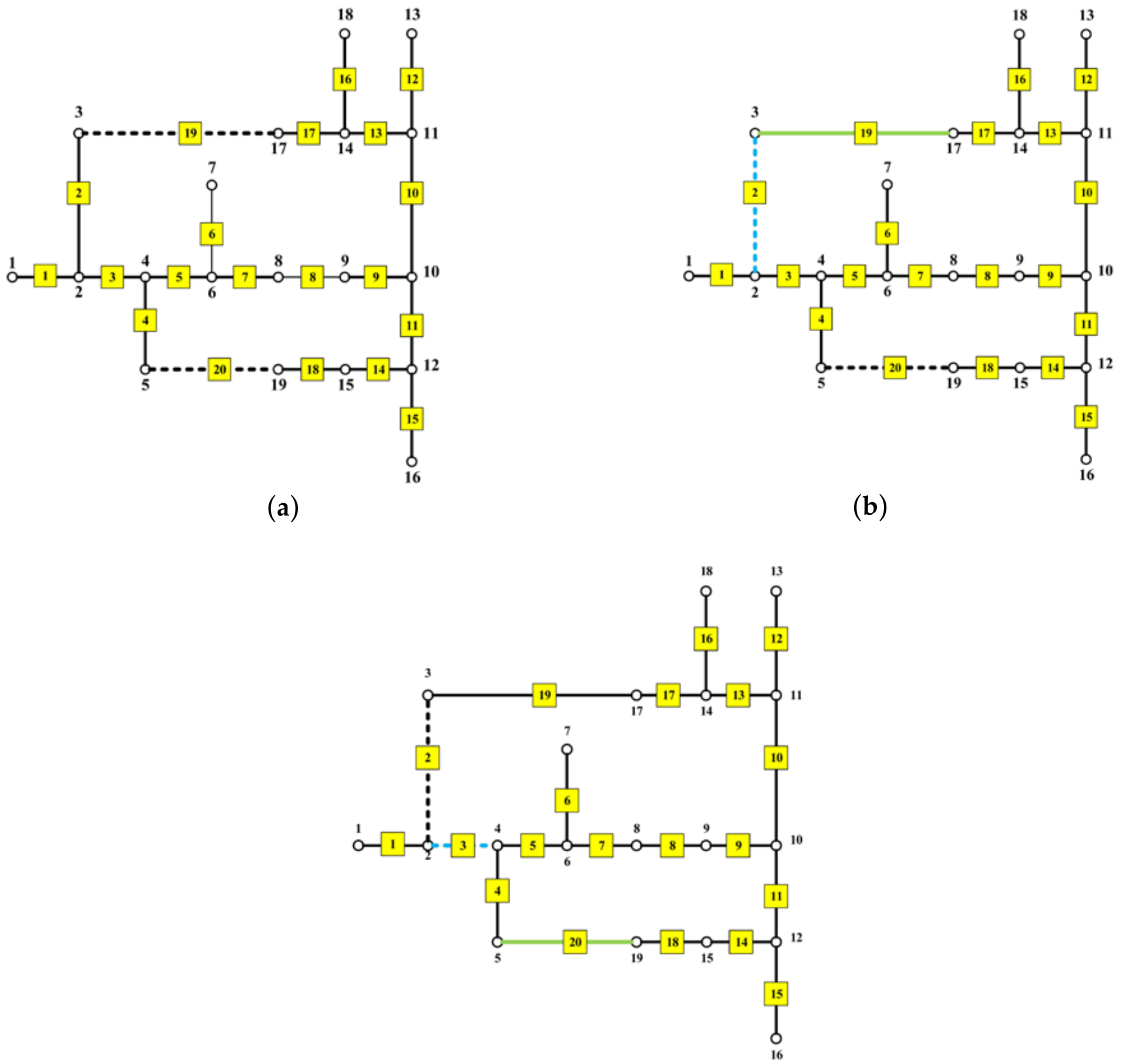

(a) (b) (c)

Figure 1. Illustrative 19-node distribution system: (a) base configuration, (b) radial configuration generated ($\boldsymbol{X}_{check}^{(0)}$), and (c) non-radial configuration generated ($\boldsymbol{X}_{check}^{(1)}$).

2.2. SOP Modeling

SOPs were first presented in 2011 [39] to provide resilience between distribution feeders. They can be integrated in distribution networks using three topologies, comprising a back-to-back (B2B) voltage source converter (VSC), static series synchronous compensator and unified power flow controller [40]. In this work, we used a B2B-VSC as the integration topology for SOPs connected to the studied systems because of its flexibility and dynamic capability to enhance the power quality. Fig. 2 shows an illustration of SOPs integration into a distribution system. To model a SOP, the main equations to model the flow of power in the network under study are expressed as follows:

$$P_{i+1} = P_i - P_{i+1}^L - r_{i,i+1} \cdot \frac{P_i^2 + Q_i^2}{|V_i|^2} \tag{1}$$

$$Q_{i+1} = Q_i - Q_{i+1}^L - x_{i,i+1} \cdot \frac{P_i^2 + Q_i^2}{|V_i|^2} \tag{2}$$

$$|V_{i+1}|^2 = |V_i|^2 - 2\left(r_{i,i+1} \cdot P_i + x_{i,i+1} \cdot Q_i\right) + \left(r_{i,i+1}^2 + x_{i,i+1}^2\right) \frac{P_i^2 + Q_i^2}{|V_i|^2} \tag{3}$$

where P_i and Q_i are the injected active and reactive powers at the i^{th} node, P_{i+1}^L and Q_{i+1}^L are the

Preprints (www.preprints.org) | NOT PEER-REVIEWED | Posted: 30 September 2019 doi:10.20944/preprints201909.0339.v1

Peer-reviewed version available at *Energies* **2019**, *12*, 4172; doi:10.3390/en12214172

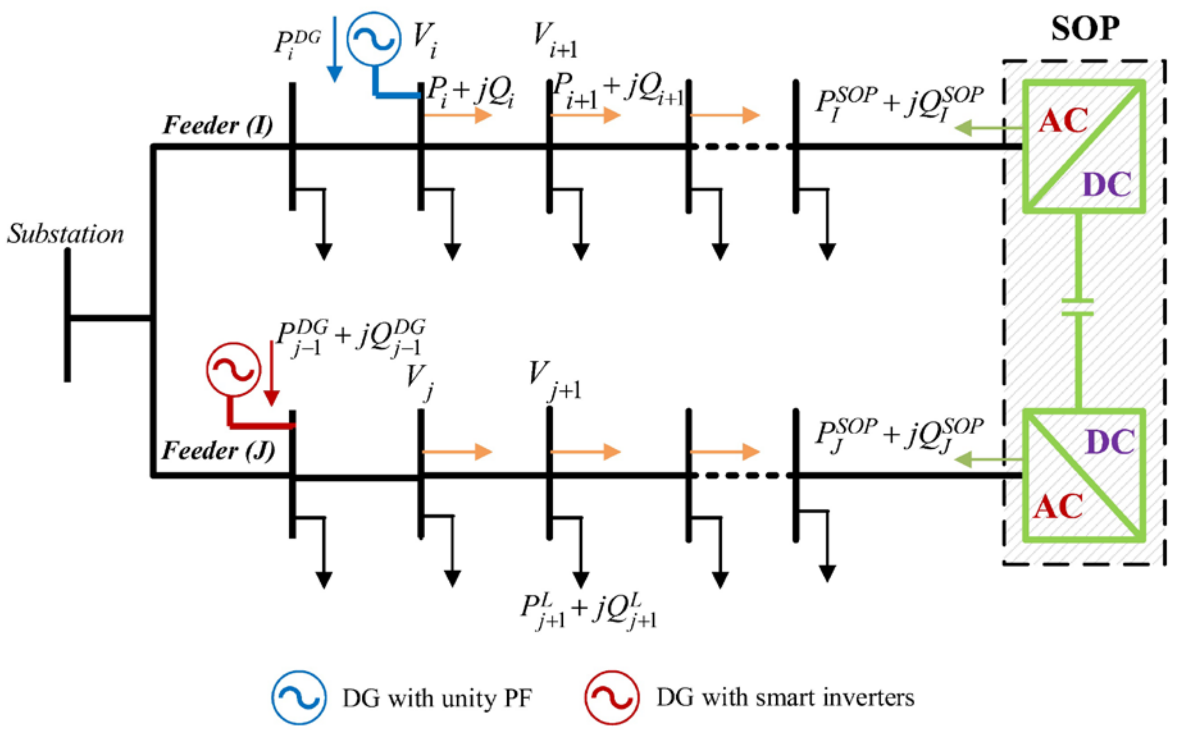

Figure 2. Illustration of SOPs integration into a distribution system

active and reactive powers of the connected loads onto node $i+1$, $|V_i|$ is the magnitude of the i^{th} node voltage and $r_{i,i+1}$ and $x_{i,i+1}$ are the feeder resistance and reactance between nodes i and $i+1$.

Then, the SOP is integrated using its active and reactive powers injected at its terminals as presented in Fig. 2, in which the summation of the injected powers at the SOP terminals and the internal power loss of its converters must equal zero, as expressed in (4). Thus:

$$P_I^{SOP} + P_J^{SOP} + P_I^{SOP-loss} + P_J^{SOP-loss} = 0 \tag{4}$$

The reactive power limits are given in (5) and the SOP capacity limit is shown in (6). Thus:

$$Q_I^{SOP-min} \le Q_I^{SOP} \le Q_I^{SOP-max}, \forall I, J \in N_f \tag{5}$$

$$\sqrt{(P_I^{SOP})^2 + (Q_I^{SOP})^2} \le S_I^{SOP}, \forall I \in N_f \tag{6}$$

where N_f is the number of feeders, P_I^{SOP} is the SOP's active power injected to the I^{th} feeder, P_J^{SOP} is the SOP's active power to the J^{th} feeder, $P_I^{SOP-loss}$ is the active power loss of the converter connected to the I^{th} feeder, $P_J^{SOP-loss}$ is the internal power loss of the converter connected to the J^{th} feeder, Q_I^{SOP} is the SOP's reactive power injected to the I^{th} feeder, Q_J^{SOP} is the SOP's reactive power injected to the J^{th} feeder, $Q_I^{SOP-min}$ and $Q_I^{SOP-max}$ are the minimum and maximum limits of the SOP's reactive power injected to the I^{th} feeder, and S_I^{SOP} is the maximum capacity limit of the planned SOP. Further, the active loss of each converter ($P_I^{SOP-loss}$ and $P_J^{SOP-loss}$) and the total SOPs active power loss ($P^{SOP-loss}$) are formulated in (7) and (8) as follows [32]:

$$P^{SOP-loss} = \sum_{I=1}^{N_f} P_I^{SOP-\ loss} \tag{7}$$

$$P_I^{SOP-loss} = A_{loss}^{SOP}\sqrt{(P_I^{SOP})^2 + (Q_I^{SOP})^2}, \forall I \in N_f \tag{8}$$

where A_{loss}^{SOP} is the loss coefficient of VSCs, which represents leakage in the transferred power to the total power transferred between feeders [32]-[34].

Mathematically, to represent the SOP variables, first, we can consider a lossless SOP, i.e. $P_I^{SOP-\ loss} = 0, \forall I \in N_f$; hence, a SOP can be represented by its injected active and reactive powers $(P_I^{SOP}, Q_I^{SOP}, Q_J^{SOP})$, where $P_J^{SOP} = -P_I^{SOP}$. Therefore, multiple SOPs can be modeled by the vector $[P_I^{SOP}(1), Q_I^{SOP}(1), Q_J^{SOP}(1), \dots P_M^{SOP}(n), Q_M^{SOP}(n), Q_K^{SOP}(n)]$ such that the first three variables in the vector represent the first SOP connected between the Ith and Jth feeders, while the last three variables represent the nth SOP connected between the Mth and Kth feeders.

Preprints (www.preprints.org) | NOT PEER-REVIEWED | Posted: 30 September 2019 doi:10.20944/preprints201909.0339.v1

Peer-reviewed version available at Energies 2019, 12, 4172; doi:10.3390/en12214172

Second, we can consider the SOP with its losses taken into account, i.e. $P_I^{SOP-loss} \neq 0, \forall I \in N_f$; hence, starting from (4), we can get $P_I^{SOP-loss}$ as follows:

$$P_J^{SOP} = -P_I^{SOP} - P_I^{SOP-loss} - P_J^{SOP-loss} \tag{9}$$

Substituting (8) into (9), then

$$P_J^{SOP} = -P_I^{SOP} - A_{loss}^{SOP}\sqrt{(P_I^{SOP})^2 + (Q_I^{SOP})^2} - A_{loss}^{SOP}\sqrt{\left(P_J^{SOP}\right)^2 + \left(Q_J^{SOP}\right)^2} \tag{10}$$

Accordingly, if we set P_I^{SOP}, Q_I^{SOP} and Q_J^{SOP} as the SOP's decision variables, (10) will be a nonlinear equation with one unknown $\left(P_J^{SOP}\right)$. So, it can be independently solved using numerical analysis methods such as Newton's method to find the value of the root (P_J^{SOP}) of (10). Therefore, assuming that A_{loss}^{SOP} is known; a SOP can be represented by its injected active and reactive powers $\left(P_I^{SOP}, Q_I^{SOP}, Q_J^{SOP}\right)$ as the lossless SOP case.

2.3. DG Modeling

In this study, we used two types of DGs. The first type includes generators with unity power factor and the second is DGs with smart inverters with a reactive power compensation capability within specified limits of the reactive power.

The DGs with unity PF are limited by the maximum capacity limit (S^{DG}) of the installed DGs as follows:

$$0 \leq P_i^{DG} \leq S^{DG} \tag{11}$$

where P_i^{DG} is the active DG power injected at the i^{th} node.

In the second type of DG, the reactive power varies based on specified PF limits, so that $-\beta_{min}$ and β_{min} are the minimum leading and lagging PF values.

$$\sqrt{(P_i^{DG})^2 + (Q_i^{DG})^2} \leq S^{DG} \tag{12}$$

$$-\tan(cos^{-1}\beta_{min}) \cdot P_i^{DG} \leq Q_i^{DG} \leq tan(cos^{-1}\beta_{min}) \cdot P_i^{DG} \tag{13}$$

where Q_i^{DG} is the reactive DG power injected at the i^{th} node.

2.4. PQ Indices

In power distribution systems, apart from the functions that describe the objective and constraints that assess the operational performance, there are other indices that evaluate the impacts of the proposed solution on the PQ performance of the studied systems, such as the load balancing index (LBI), and aggregate voltage deviation index ($AVDI$). The mathematical expressions for these quantities are given as follows:

2.4.1. Load Balancing Index (LBI)

Changing the state of the switches of a distribution system will change its topography. In turn, the loads between the feeders can be distributed to balance the system and avoid the overloading of feeders. In this work, the balancing index (LBI) is used to reflect the loading level of each line in the distribution network [15]. The LBI of the b^{th} line is formulated as follows:

$$LBI_b = \left(\frac{I_b}{I_b^{rated}}\right)^2, \forall b \in N_{br} \tag{14}$$

where I_b is the current flowing in line b and is limited by its rated value I_b^{rated} and N_{br} is the number of lines. Hence, the total load balancing index LBI_{tot} is expressed as the sum of the balancing indices of the lines, thus:

$$LBI_{tot} = \sum_{b=1}^{N_{br}} LBI_b \tag{15}$$

LBI of a certain line decreases if the total load connected to this line decreases, and hence, the line current decreases. However, line currents may increase in other lines, increasing their LBIs. For that, the LBI_{tot} is calculated for all branches to help determine the overall load balancing of all lines in the distribution network.

Preprints (www.preprints.org) | NOT PEER-REVIEWED | Posted: 30 September 2019 doi:10.20944/preprints201909.0339.v1

Peer-reviewed version available at Energies 2019, 12, 4172; doi:10.3390/en12214172

2.4.2. Aggregate voltage deviation index *(AVDI)*

Voltage deviation is a measure of the voltage quality in the system. It is formulated as the summation of voltage deviations at all nodes in the system from a reference value of 1 per unit, and it is given as:

$$AVDI = \sum_{i=1}^{N_n} |V_i - 1| \tag{16}$$

where i and N_n are the node number and total number of nodes, respectively. A system with lower $AVDI$ indicates a secure system with reduced voltage violations.

3. Problem Statement

3.1. Objective Function

The main aim of this work is to minimize the total power loss (P_{loss}^{tot}). The objective function P_{loss}^{tot} is divided into two parts, namely the feeder losses due to current flowing in the lines and the SOP's internal power loss ($P^{SOP-loss}$) as expressed in (17).

$$Min\ P_{loss}^{tot} = \sum_{i=1}^{N_n} \left(\frac{P_i^2 + Q_i^2}{|V_i|^2} \cdot r_{i,i+1} \right) + \mu \cdot P^{SOP-loss} \tag{17}$$

where μ=0 with no SOP losses considered and μ=1 if SOP losses are considered.

3.2. Constraints and Operation Conditions

In addition to the radiality requirements described in Section II. A, power flow equality given in (4), SOP reactive power limits given in (5), SOP capacity limit given in (6), SOP active power loss given in (8), DG capacity limit given in (11) for the first type and (12) for the second type, and DG reactive power limits given in (13), the following constraints regarding voltage magnitudes, lines thermal capacities and the total reactive power injected by DGs and/or SOPs into the system are expressed, respectively, as follows:

$$V_{min} \leq |V_i| \leq V_{max} \tag{18}$$

$$|I_b| \leq I_b^{rated}, \forall b \in N_{br} \tag{19}$$

$$\sum_{i=1}^{N_{DG}} Q_i^{DG} + \sum_{k=1}^{N_{SOP}} \left(Q_I^{SOP}(k) + Q_J^{SOP}(k) \right) \leq \sum_{u=1}^{N_n} Q_u^L \tag{20}$$

where V_{min} and V_{max} represent minimum and maximum voltage limits respectively, and N_{DG} is the number of connected DGs. It should be noted that the total reactive power injected by DGs and SOPs must not exceed the total demand reactive power, as expressed in (20), to avoid the system's over-compensation, and to maintain the PF to be within higher lagging values [35], [36]. Also, no reverse power flow is permitted in the system, as expressed in (21). Otherwise, further precautions should be taken by network operators to control excessive reverse power flows and the associated problems resulting from high DG penetration levels.

$$P_i^L - a \cdot P_i^{DG} - b \cdot P_I^{SOP} - c \cdot P_J^{SOP} \geq 0, \forall i \in N_n \tag{21}$$

where a equals 1 in the case of node i connected to a DG unit, b equals 1 in the case of node i connected to a SOP through feeder I, and c equals 1 in the case of node i connected to a SOP through feeder J; otherwise, $a = b = c = 0$.

3.3. Search Algorithm

The hyper-spherical search (HSS) algorithm was developed by Karami *et al.* in 2014 [37] to solve nonlinear functions and was further enhanced in 2016 [38] to consider mixed continuous-discrete decision variables to solve MINLP problems. The DC-HSS has the advantages of fast convergence to the optimal/near-optimal solutions and good performance in solving mixed continuous-discrete problems. Therefore, we have used the DC-HSS algorithm to solve our optimization problem.

3.3.1. Continuous HSS

Preprints (www.preprints.org) | NOT PEER-REVIEWED | Posted: 30 September 2019 doi:10.20944/preprints201909.0339.v1

Peer-reviewed version available at Energies 2019, 12, 4172; doi:10.3390/en12214172

The population is categorized into two types: particles and sphere-centers (SCs). The algorithm searches in the inner space of the hyper-sphere to find a new particle position with a better value of the objective function as follows:

Step 1: Initialization: the algorithm starts by assigning the population size (N_{pop}), the distance between the particle and the sphere-center (r), taking into account random values between $[r_{min}, r_{\max}]$, the number of sphere-centers (N_{SC}), the number of decision variables (N), the probability of changing the particle's angle (Pr_{angle}), and the maximum number of iterations (Max_{iter}). Then, a vector of decision variables (x_i) is initialized with random values between $[X_{i_{min}}, X_{i_{\max}}]$ by a uniform probability function. A set equal to N_{pop} containing the objective function values is formed for each vector, in which each vector of the decision variables $[x_1, x_2, \dots, x_N]$ is named as a particle. Further, the particles are sorted according to their objective function values, and then the best N_{SC} particles with the lowest objective function are selected as the initial sphere-centers. The rest of the particles $(N_{pop} - N_{SC})$ are then distributed among the sphere-centers. Finally, a distribution of the $(N_{pop} - N_{SC})$ particles among the SCs is performed by the objective function difference (OFD) for each SC, where the OFD is equal to the objective function of SC (f_{SC}) subtracted from the maximum objective value of SCs $(OFD = f_{SC} - \max_{SCs} f)$. The normalized dominance for each SC is defined as:

$$D_{SC} = \left| \frac{OFD_{SC}}{\sum_{i=1}^{N_{SC}} OFD_i} \right| \tag{22}$$

A randomly chosen $round\{D_{SC} \times (N_{pop} - N_{SC})\}$ number of particles is assigned to each SC.

Step 2: Searching: each particle seeks to find a better solution by searching the bounding sphere whose center is the assigned SC. The radius of this sphere is r. The particle parameters $(r \text{ and } \theta)$ are changed to perform the searching procedure as shown in Fig. 3. The dashed space in Fig. 3 shows the possible positions for a particle. The angle of the particle is changed by $\propto$, which ranges between $(0,2\pi)$ with a probability equal to Pr_{angle}. For each particle, r is changed between $[r_{min}, r_{\max}]$, where $r_{\max}$ can be calculated from (23):

$$r_{\max} = \sqrt{\sum_{i=1}^{N} \left(x_{i,SC} - x_{i,particle}\right)^2} \tag{23}$$

After the search for particles, if a new particle position has a lower objective function value than that of its SC, both the SC and particle will exchange their roles, *i.e.* the particle becomes the new SC and the old SC becomes the new particle.

Step 3: Dummy particles recovery: An SC with its particles forms a set of particles.

The values of the set objective function (SOF) for each set of particles sort these sets to find the worst sets, in which dummy (inactive) particles are located. The SOF is given by (24).

$$SOF = f_{SC} + \left(\gamma \cdot mean\{f_{particles\ of\ SC}\}\right) \tag{24}$$

where γ is scalar. If γ is small, SOF will be biased towards f_{SC}, otherwise, SOF will be biased towards $f_{particles\ of\ SC}$.

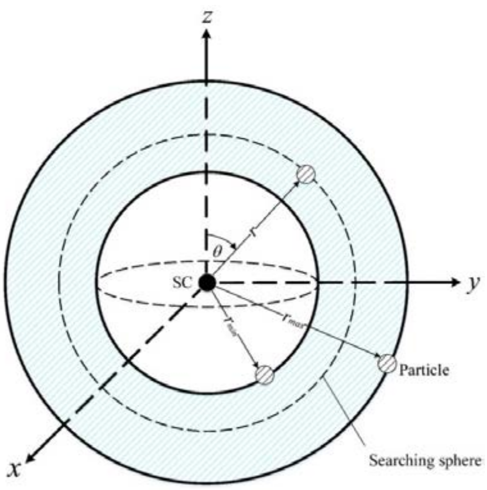

Figure 3. Sphere-center and particle positions indicated by the dashed space

Preprints (www.preprints.org) | NOT PEER-REVIEWED | Posted: 30 September 2019 doi:10.20944/preprints201909.0339.v1

Peer-reviewed version available at *Energies* **2019**, *12*, 4172; doi:10.3390/en12214172

To assign dummy particles to other SCs, two parameters are calculated: the first parameter represents the difference of SOF ($DSOF$) for each set and the second one represents the assigning probability (AP) for each SC. These parameters are expressed as follows:

$$DSOF = SOF - \max_{groups} \{SOF\ of\ groups\} \tag{25}$$

$$AP = [AP_1, AP_2, \dots \dots, AP_{N_{SC}}] \tag{26}$$

Further, a preset number of particles N_{newpar} with the worst function values are exchanged with the new generated N_{newpar} particles. Hence, after several iterations, the particles and their SCs will become close.

Step 4: Termination: the termination criterion is fulfilled if the number of iterations reaches its Max_{iter} or the difference between the function values of the best SCs is smaller than a pre-set tolerance value.

3.3.2. Discrete HSS

Like the continuous HSS, the discrete HSS starts with the initialization of particles, but with discrete variables. Solutions are then generated randomly from the discrete variables $(X_{id,min}, X_{id,min} + 1, \dots, X_{id,max} - 1, X_{id,max})$ with a uniform probability. N_{SC} particles with the lowest function values are assigned as SCs. The rest of the particles are distributed among the SCs. Then, the same searching procedure as the continuous HSS is performed. It should be mentioned that the angle $\propto$ is not considered in the searching procedure of the discrete HSS and the only parameter used is the radius r_d, where r_d is selected between $(r_{d,min}, r_{d,min} + 1, \dots, r_{d,max} - 1, r_{d,max})$. $r_{d,max}$ is calculated as follows:

$$r_{d,max} = \sqrt{\sum_{i=1}^{N} \left(x_{i_d,SC} - x_{i_d,particle}\right)^2} \tag{27}$$

The other steps will be performed as presented in the continuous HSS algorithm.

3.3.3. Discrete-continuous HSS (DC-HSS)

DC-HSS combines both continuous and discrete HSS algorithms, in which the particles contain both continuous and discrete variables. The procedure for the continuous variables is structured as presented in the continuous HSS formulation, whilst the procedure for the discrete variables is structured as presented in the discrete HSS formulation. To sum up, the optimization parameters of DC-HSS are as follows: N_{pop}=1000, $N_{SC} = 100$, $r_{min} = 0$, $r_{\max} = 1$, $r_{d,min} = 0$, $r_{d,max} = 1$, $N_{newpar} = 5$, $Pr_{angle} = 75\%$ and $Max_{iter} = 1000$. Fig. 4 illustrates a comprehensive flowchart for the proposed problem formulation using the DC-HSS algorithm.

3. Problem Statement

In this section, the results obtained in the nine scenarios are presented for IEEE 33-node and 83-node systems under different loading conditions. Further, the contribution of SOP loss to the total active power loss as well as the effect of increasing the number of SOPs connected to the systems are studied. Case studies are carried out on an Intel Core i7 CPU, second generation, at 2.2 GHz and 3 GHz maximum turbo boost speed, with 6 GB of RAM with speed 1333 MHz, 6 MB cache memory and contains SSD hard disk at 550 MB per second.

3.1. IEEE 33-node distribution system

The IEEE 33-node base configuration consists of 32 sectionalized lines and 5 tie-lines as shown in Fig. 5. The number of SOPs that can be installed ranges from 1 to 5, *i.e.* $N_{SOP} \in [1,5]$, where the individual SOP rating ($S_I^{SOP} = S_J^{SOP}$) is 1 MVA and A_{loss}^{SOP} equals 0.02 [32], [41], [42]. N_{DG} is set to 3 while S^{DG}equals 1 MVA with unity PF. V_{min} and V_{max} values are 0.95 and 1.05 p.u., respectively. Also, I_b^{rated} is set to 300 A.

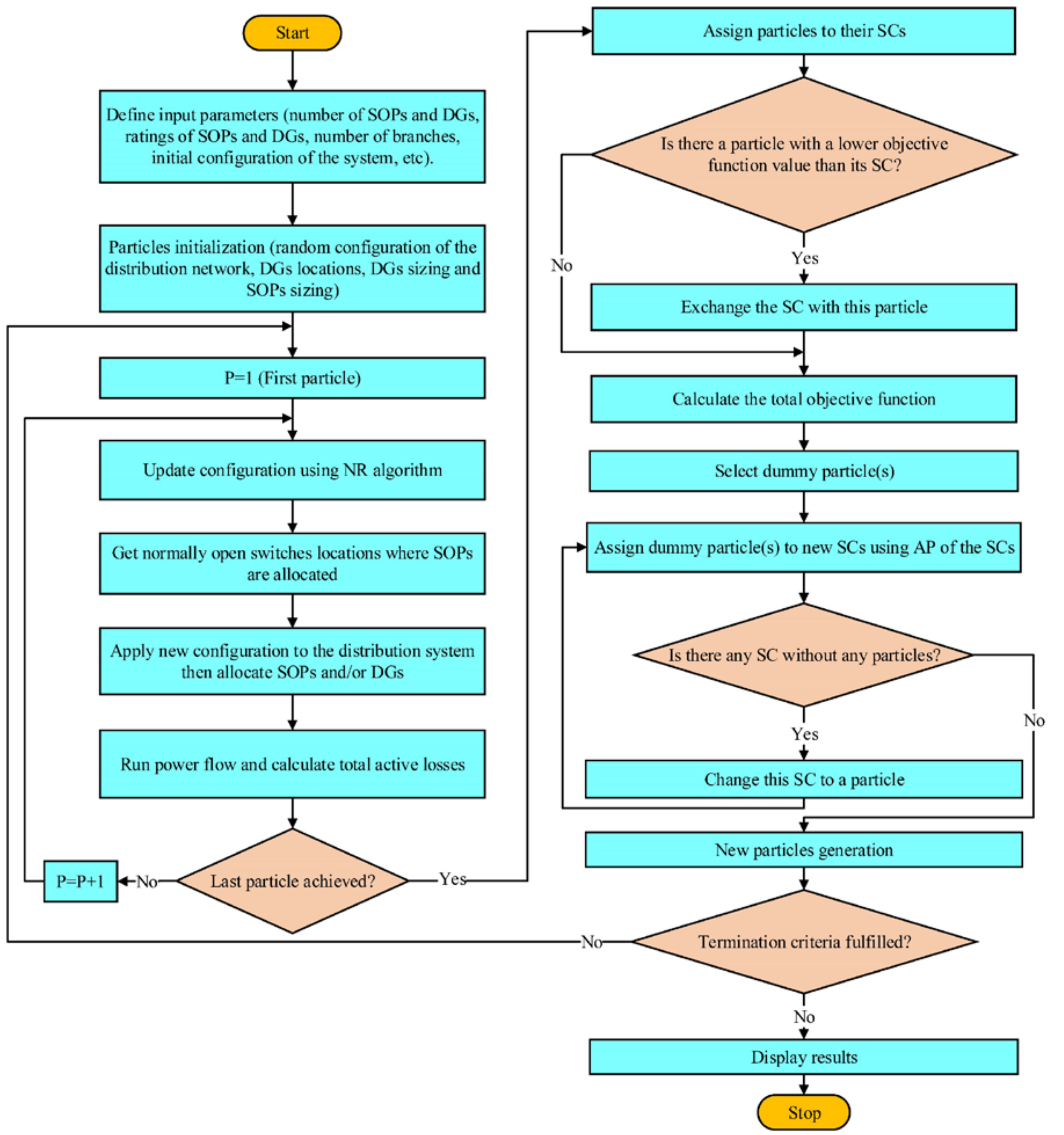

Figure 4. A comprehensive flowchart for the proposed problem formulation using the DC-HSS algorithm

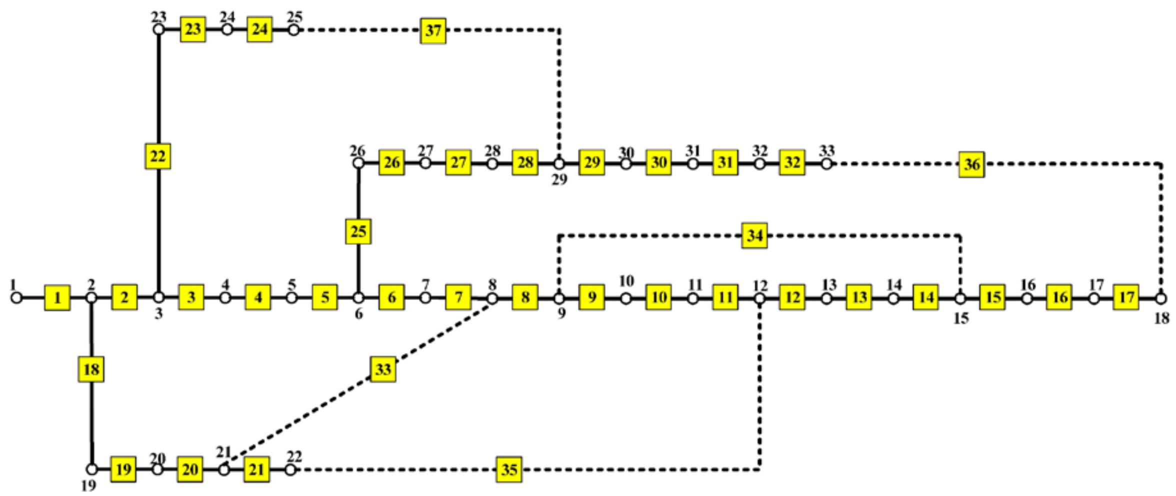

Figure 5. IEEE 33-node distribution system

Preprints (www.preprints.org) | NOT PEER-REVIEWED | Posted: 30 September 2019 doi:10.20944/preprints201909.0339.v1

Peer-reviewed version available at *Energies* **2019**, *12*, 4172; doi:10.3390/en12214172

First, the results obtained for the system in the first three scenarios with no SOPs installed are given in Table 3.

Table 3

Total power losses and PQ indices for scenarios 1, 2 and 3: IEEE 33-node system

Loading level	Scenario	P_{loss}^{tot} (kW)	LBI_{tot}	$AVDI$
Light (50%)	1	33.646	0.058	0.678
	2	41.212	0.376	0.862
	3	21.346	0.178	0.500
Normal (100%)	1	NA		
	2			
	3	90.013	0.765	1.064
Heavy (160%)	1	NA		
	2			
	3			

On the one hand, the results clarify that optimizing the NR and DGs allocation strategies separately cannot satisfy the voltage requirements in either the normal or heavy loading conditions, and only a sub-optimal performance can be achieved in the light loading case. On the other hand, simultaneous NR and DGs allocation can meet the problem limits in light and normal loading conditions only. Hence, one can conclude that the first three scenarios cannot guarantee acceptable performance level of the IEEE 33-node system with loads alteration.

Second, the results obtained for scenarios 4 to 9 with lossless SOPs installed in the system are presented in Table 4 under the three loading conditions.

Table 4. Total Power Losses and PQ Indices for Scenarios 4 to 9 with Lossless SOPs Installed: IEEE 33-node system

Scenario	N_{SOP}	Light loading (50%)			Normal loading (100%)			Heavy loading (160%)		
		P_{loss}^{tot} (kW)	LBI_{tot}	$AVDI$	P_{loss}^{tot} (kW)	LBI_{tot}	$AVDI$	P_{loss}^{tot} (kW)	LBI_{tot}	$AVDI$
4	1	38.723	0.343	0.745	NA			NA		
	2	33.686	0.303	0.709						
	3	32.097	0.292	0.701	144.337	1.285	1.085			
	4	29.481	0.271	0.603	143.107	1.255	0.973			
	5	27.420	0.252	0.572	128.576	1.145	1.093			
5	1	23.936	0.211	0.565	NA			NA		
	2	22.323	0.199	0.427	91.206	0.823	0.928			
	3	22.613	0.204	0.444	93.576	0.842	0.969			
	4	22.028	0.205	0.413	89.932	0.833	0.877	269.511	2.317	0.977
	5	22.323	0.209	0.403	89.942	0.832	0.830	267.975	2.275	1.081
6	1	23.709	0.215	0.536	98.803	0.897	1.126	NA		
	2	22.689	0.202	0.464	90.777	0.824	0.931			
	3	23.384	0.213	0.502	90.303	0.839	0.914	254.480	2.228	1.281
	4	22.586	0.205	0.443	89.092	0.823	0.882	255.053	2.255	1.239
	5	23.961	0.204	0.399	89.429	0.853	0.848	258.36	2.220	1.141
7	1	20.548	0.179	0.583	NA			NA		
	2	20.548	0.179	0.583						
	3	19.796	0.175	0.524	87.745	0.759	1.142			

Scenario	N_{SOP}	Light loading (50%) P_{loss}^{tot} (kW)	LBI_{tot}	$AVDI$	Normal loading (100%) P_{loss}^{tot} (kW)	LBI_{tot}	$AVDI$	Heavy loading (160%) P_{loss}^{tot} (kW)	LBI_{tot}	$AVDI$
	4	19.454	0.172	0.546	77.212	0.681	1.076			
	5	17.884	0.162	0.512	73.512	0.670	1.050			
8	1	15.299	0.121	0.495		NA			NA	
	2	13.760	0.114	0.428	55.498	0.461	0.822	153.348	1.262	1.261
	3	13.674	0.114	0.443	54.750	0.464	0.785	142.402	1.217	1.221
	4	14.503	0.123	0.416	56.238	0.482	0.798	166.628	1.478	1.302
	5	14.565	0.129	0.387	52.306	0.456	0.764	170.249	1.358	1.141
9	1	14.269	0.122	0.433	57.851	0.508	0.752	160.812	1.412	1.303
	2	13.840	0.118	0.373	51.748	0.445	0.742	144.826	1.265	1.165
	3	13.295	0.116	0.359	49.954	0.448	0.653	125.768	1.133	1.066
	4	**11.869**	0.110	0.312	50.176	0.444	0.634	137.325	1.241	1.091
	5	12.087	0.106	0.353	**45.885**	0.433	0.601	**122.062**	1.131	1.034

On the one hand, the results obtained with one SOP installed in the system with or without NR in the case of no DGs connected exhibit poor performance, which can be explained by the lack of getting an acceptable solution to the problem because of minimum voltage value violation under both the normal and heavy loading conditions, as shown in scenarios 4 and 5. Therefore, to meet the minimum voltage requirement, the reactive power should be compensated by installing additional SOPs, as presented in scenario 6, with 3 to 5 SOPs when NR was considered. On the other hand, the results obtained when DGs were connected into the system without NR (scenario 7) decreased the need for an increasing number of installed SOPs. Further, when NR is enabled, an additional reduction of the number of SOPs is noticed, which will result in reducing the power losses, as revealed by the proposed scenario 9 because it allows freedom in locating SOPs.

To sum up, the results obtained for scenario 9 (simultaneous NR with DGs and SOPs allocation) resulted in the best solutions, highlighted in bold in Table 4, with 5 SOPs at the normal and heavy loading levels and 4 SOPs at the light loading level compared to the results obtained by the other scenarios, in which the power losses are reduced by 74.787% at normal, 77.362% at light, and 78.788% at heavy loading levels with respect to the corresponding base system values. Also, the improvement of the voltage profile obtained in scenario 9 for the system at the normal loading condition is shown in Fig. 6.

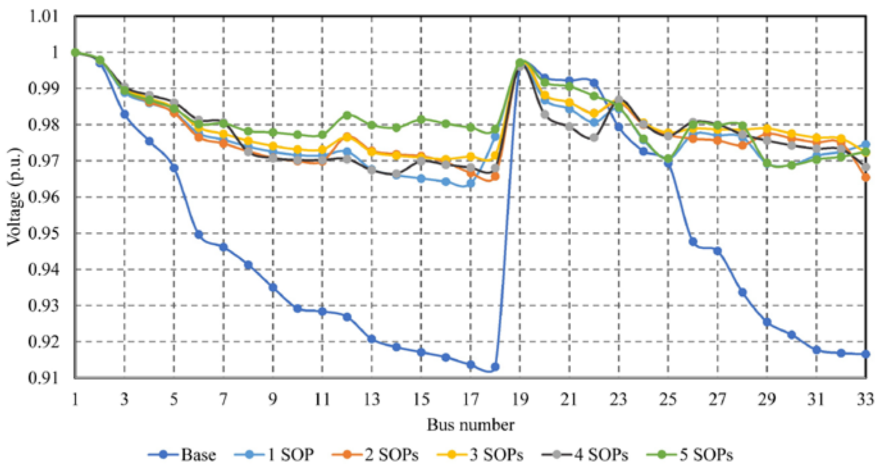

Figure 6. Improvement of the voltage profile at normal loading condition: scenario 9

Thirdly, the results obtained for scenarios 4 to 9 with the SOPs' internal power losses considered are presented in Table 5 at the three loading levels.

Preprints (www.preprints.org) | NOT PEER-REVIEWED | Posted: 30 September 2019 doi:10.20944/preprints201909.0339.v1

Peer-reviewed version available at *Energies* **2019**, *12*, 4172; doi:10.3390/en12214172

Table 5. Total Power Losses and PQ Indices for Scenarios 4 to 9 with SOP Losses Considered: IEEE 33-node system

Scenario	N_{SOP}	Light loading (50%)			Normal loading (100%)			Heavy loading (160%)		
		P_{loss}^{tot} (kW)	LBI_{tot}	$AVDI$	P_{loss}^{tot} (kW)	LBI_{tot}	$AVDI$	P_{loss}^{tot} (kW)	LBI_{tot}	$AVDI$
4	1	45.414	0.376	0.859		NA				
	2	45.796	0.361	0.819						
	3	35.479	0.292	0.699	177.087	1.099	1.042		NA	
	4	35.083	0.281	0.641	133.125	1.057	1.194			
	5	39.932	0.289	0.635	162.892	1.093	1.049			
5	1	27.184	0.219	0.572		NA				
	2	27.185	0.219	0.573	110.805	0.925	1.147		NA	
	3	30.747	0.209	0.533	113.375	0.887	1.100			
	4	37.655	0.221	0.445	126.837	0.964	0.887	415.433	2.497	0.811
	5	38.209	0.282	0.537	165.753	0.938	1.047	461.002	2.689	0.751
6	1	26.753	0.212	0.526	106.317	0.921	1.125		NA	
	2	26.753	0.212	0.526	104.076	0.881	1.015			
	3	26.754	0.212	0.525	104.774	0.858	0.934	427.952	2.525	1.283
	4	26.824	0.205	0.456	106.070	0.897	1.060	386.968	2.338	1.216
	5	29.629	0.220	0.544	119.559	0.915	1.058	377.700	2.295	1.166
7	1	23.883	0.188	0.592						
	2	27.727	0.201	0.659						
	3	27.669	0.209	0.609		NA			NA	
	4	29.336	0.213	0.632						
	5	36.100	0.234	0.579	114.118	0.783	1.123			
8	1	18.489	0.129	0.502		NA			NA	
	2	18.489	0.129	0.501	68.064	0.509	0.899	204.716	1.131	1.239
	3	19.670	0.118	0.417	72.782	0.494	0.853	196.995	1.279	1.249
	4	29.082	0.129	0.385	86.147	0.508	0.966	317.274	1.712	1.309
	5	25.052	0.129	0.336	94.222	0.578	0.769	220.982	1.289	1.189
9	1	16.828	0.126	0.441	67.019	0.525	0.911		NA	
	2	**16.575**	0.119	0.375	**66.131**	0.527	0.804	193.316	1.362	1.322
	3	17.144	0.126	0.446	73.735	0.483	0.782	189.168	1.352	1.238
	4	20.329	0.127	0.390	74.077	0.500	0.746	193.753	1.211	1.029
	5	19.819	0.118	0.408	74.695	0.469	0.602	**188.831**	1.176	1.135

Regardless of economic aspects, in the lossless SOP scenarios, the system with an increased number of installed SOPs becomes more efficient because of the considerable power loss reduction. However, this is not the case if the SOPs' internal losses are considered, because power loss minimization is considerably affected by the SOPs internal losses. This makes clear that loss minimization is not guaranteed by installing more SOPs. In addition, one cannot simply suppose that increasing the number of installed SOPs will increase the SOPs' internal losses proportionally, as this depends on the power transferred by the SOPs and also on the SOPs' locations, as clarified in Fig. 7, with results obtained in scenario 9 that make clear that choosing an appropriate number of SOPs is a matter of optimization. Moreover, after considering the internal power losses of the SOPs, it is obvious that the results obtained for scenario 9 are the best results obtained so far compared to the results obtained for the other scenarios, in which the power losses are reduced by 67.374% using two

Preprints (www.preprints.org) | NOT PEER-REVIEWED | Posted: 30 September 2019 doi:10.20944/preprints201909.0339.v1

Peer-reviewed version available at *Energies* **2019**, *12*, 4172; doi:10.3390/en12214172

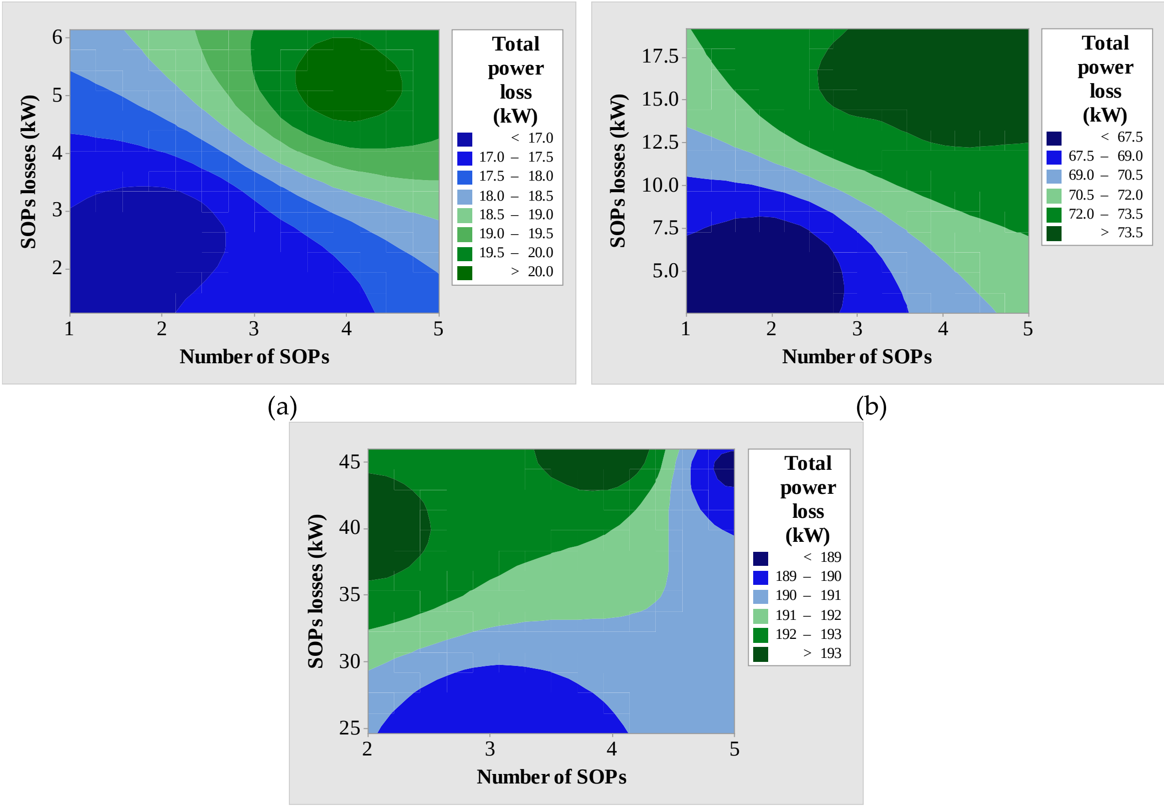

Figure 7. Contour plots of total power loss versus SOPs losses and N_{SOP}: (a) light loading, (b) normal loading, and (c) heavy loading.

SOPs at normal, 64.374% using two SOPs at light, and 67.184% using five SOPs at heavy loading levels. All values are given with respect to the corresponding base system values. Furthermore, all the considered PQ indices are enhanced using the same scenario by different values as presented in Table 5, which validates the effectiveness of the proposed solution. The improvement of the voltage profile obtained in scenario 9 for the system at the normal loading condition with the SOPs' power loss considered is shown in Fig. 8. A detailed summary of the optimal results obtained for scenarios 4 to 9 at the normal loading condition is given in Tables A.1 and A.2 in the Appendix. Also, the IEEE 33-node system after applying scenario 9 at normal loading condition is shown in Fig. 12. Finally, optimizing the NR, DGs and SOPs allocation strategies collectively facilitates collaboration between strategies, which will enable the best performance level of the system to be achieved.

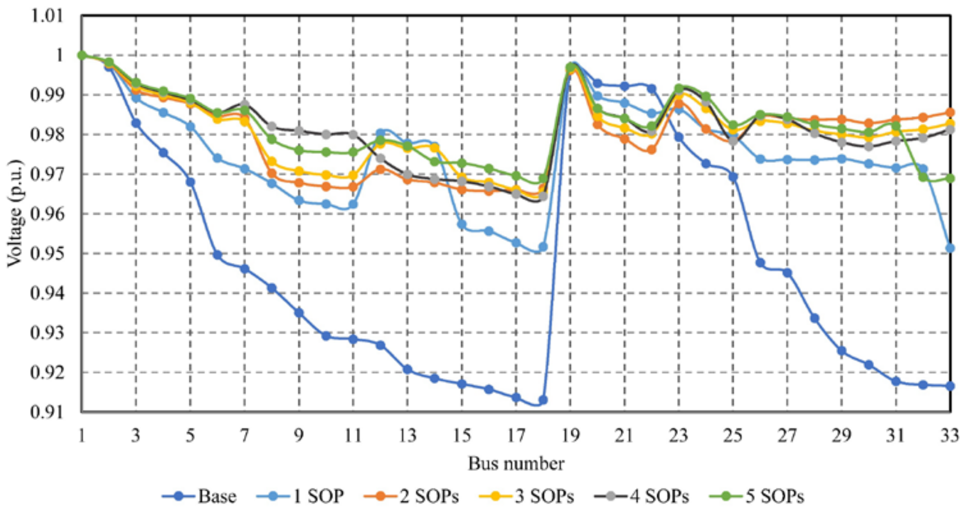

Figure 8. Improvement of the voltage profile at normal loading condition with SOPs power loss considered: scenario 9

3.2. 83-node distribution system

In order to validate the effectiveness of scenario 9 proposed in this work, it was examined on an 83-node balanced distribution system from a power company in Taiwan, in which the 83-node base configuration consists of 83 sectionalized lines and 13 tie-lines as shown in Fig. 9. The number of SOPs that can be installed ranges from 1 to 5, i.e. $N_{SOP} \in [1,5]$, where the individual SOP rating ($S_i^{SOP} = S_j^{SOP}$) is 1.5 MVA and A_{loss}^{SOP} equals 0.02 [32], [41], [42]. N_{DG} is set to 8 with S^{DG}equal to 3 MVA and PF ranges from 0.95 lagging to unity. The V_{min} and V_{max} values are 0.95 and 1.05 p.u., respectively. Also, I_b^{rated} is set to 310 A.

First, the results obtained for the system in the first three scenarios with no SOPs installed in the system are given in Table 6. Once more, the results make clear that optimizing the NR and DGs allocation strategies separately cannot satisfy the voltage requirements at the heavy loading level, and only a sub-optimal performance can be achieved at the light and normal loading levels. However, simultaneous NR and DGs allocation can meet the problem limits considered in the normal and light loading conditions only.

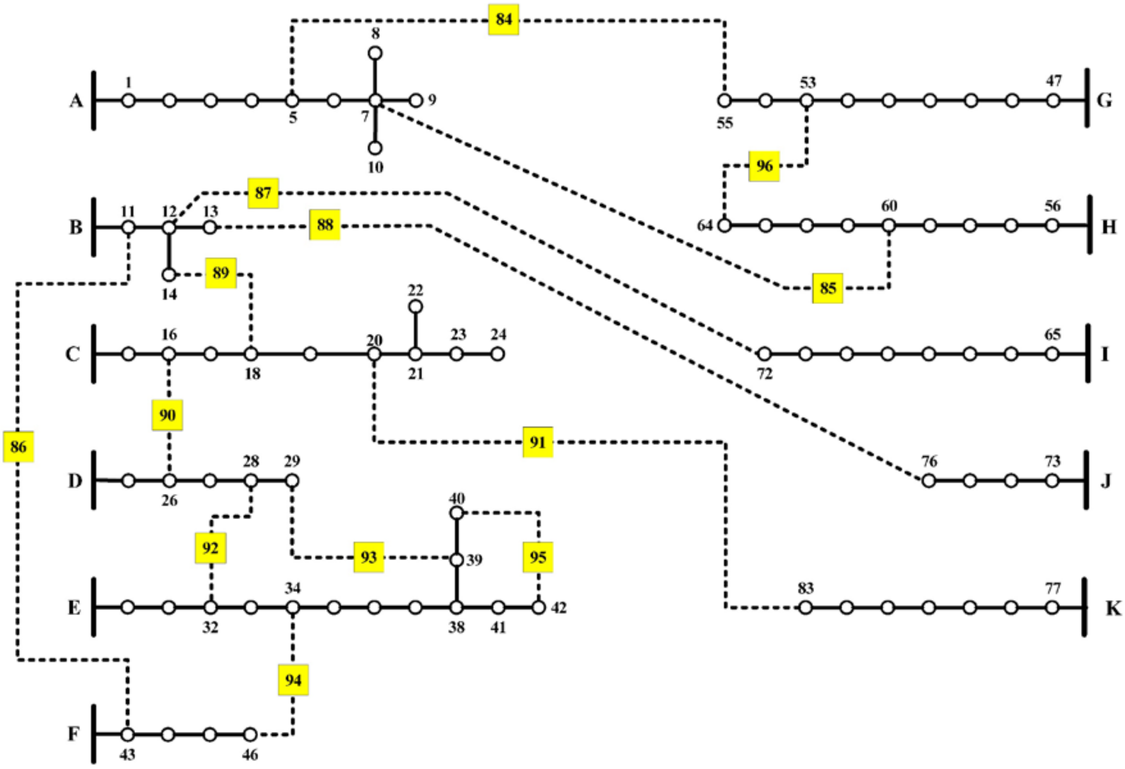

Figure 9. The 83-node distribution system

Table 6. Total power losses and PQ indices for scenarios 1, 2 and 3: 83-node system

Loading level	Scenario	P_{loss}^{tot} (kW)	LBI_{tot}	$AVDI$
Light (50%)	1	113.382	3.237	1.303
	2	97.496	2.713	1.249
	3	87.033	2.425	1.128
Normal (100%)	1	470.241	13.259	2.654
	2		NA	
	3	368.364	10.699	2.309
Heavy (130%)	1			
	2		NA	
	3			

Preprints (www.preprints.org) | NOT PEER-REVIEWED | Posted: 30 September 2019 doi:10.20944/preprints201909.0339.v1

Peer-reviewed version available at *Energies* **2019**, *12*, 4172; doi:10.3390/en12214172

Second, the results obtained for scenarios 4 to 9 with/without SOPs internal losses in the system are presented in Tables 7 and 8 at the three loading levels.

Table 7. Total power losses and PQ indices for scenarios 4 to 9 without SOP losses: 83-node system

Scenario	N_{SOP}	Light loading (50%)			Normal loading (100%)			Heavy loading (130%)		
		P_{loss}^{tot} (kW)	LBI_{tot}	$AVDI$	P_{loss}^{tot} (kW)	LBI_{tot}	$AVDI$	P_{loss}^{tot} (kW)	LBI_{tot}	$AVDI$
4	1	112.236	3.035	1.163						
	2	107.777	2.929	0.976						
	3	106.452	2.911	0.847		NA				
	4	98.345	2.662	0.958						
	5	99.079	2.697	0.779						
5	1	106.662	3.000	1.213	441.694	12.273	2.501			
	2	103.194	2.898	1.137	427.829	12.010	2.373			
	3	104.861	2.945	1.029	421.891	11.660	2.297		NA	
	4	101.766	2.773	1.062	412.534	11.248	2.171			
	5	96.026	2.769	0.811	390.587	11.017	1.893			
6	1	105.558	3.014	1.034	442.042	12.584	2.293			
	2	100.563	2.878	0.969	425.271	12.106	2.229			
	3	96.450	2.747	0.823	405.221	11.232	2.137			
	4	92.742	2.661	0.825	385.354	10.501	1.836			
	5	89.949	2.484	0.696	407.074	10.428	2.109			
7	1	54.413	1.511	0.895	231.704	6.396	1.879	439.890	12.036	2.773
	2	54.935	1.511	0.887	226.485	6.284	1.614	387.021	10.649	2.325
	3	52.594	1.496	0.680	214.617	6.000	1.668	394.187	10.901	2.233
	4	49.215	1.382	0.688	192.775	5.519	1.464	371.243	10.239	2.214
	5	52.882	1.512	0.632	197.090	5.579	1.562	333.774	9.363	1.816
8	1	60.405	1.797	1.019	253.559	7.358	2.019			
	2	58.648	1.755	0.928	240.294	7.059	1.925			
	3	62.326	1.822	0.899	249.926	7.224	1.979		NA	
	4	57.268	1.679	0.879	243.006	6.816	1.795			
	5	54.513	1.681	0.723	210.822	6.284	1.584			
9	1	51.425	1.456	0.792	219.131	6.282	1.713	379.446	10.806	2.345
	2	49.481	1.382	0.667	203.24	5.821	1.550	345.422	10.022	1.997
	3	46.868	1.321	0.641	192.115	5.392	1.463	348.556	9.905	2.196
	4	**43.469**	1.238	0.587	189.128	5.084	1.379	345.018	10.815	2.080
	5	45.122	1.309	0.566	**189.073**	5.140	1.386	**302.561**	9.163	1.571

From Tables 7 and 8, it can be observed that installing SOPs without NR optimization and DGs allocation (scenario 4) failed to operate the system within the specified limits, even after increasing the number of SOPs. On the one hand, for the lossless SOPs cases, scenario 7 succeeded in finding acceptable solutions for the problem, contrary to scenarios 4, 5, 6 and 8, all of which failed to find an acceptable solution even with an increased number of SOPs. On the other hand, taking SOPs losses

Preprints (www.preprints.org) | NOT PEER-REVIEWED | Posted: 30 September 2019 doi:10.20944/preprints201909.0339.v1

Peer-reviewed version available at *Energies* **2019**, *12*, 4172; doi:10.3390/en12214172

Table 8. Total power losses and PQ indices for scenarios 4 to 9 with SOP losses considered: 83-node system

Scenario	N_{SOP}	Light loading (50%)			Normal loading (100%)			Heavy loading (130%)		
		P_{loss}^{tot} (kW)	LBI_{tot}	$AVDI$	P_{loss}^{tot} (kW)	LBI_{tot}	$AVDI$	P_{loss}^{tot} (kW)	LBI_{tot}	$AVDI$
4	1	126.023	3.313	1.349						
	2	134.346	3.219	1.060						
	3	139.039	3.364	1.201		NA				
	4	144.968	3.049	1.279						
	5	145.084	2.893	1.090						
5	1	117.084	3.250	1.287	473.623	12.788	2.610			
	2	119.178	3.170	1.267	478.019	12.783	2.568			
	3	133.988	3.187	1.227	491.723	12.480	2.504			
	4	142.552	2.934	1.188	512.955	12.595	2.374			
	5	145.349	3.024	1.156	518.085	11.919	2.181			
6	1	114.048	3.263	1.278	472.069	13.065	2.646			
	2	116.980	3.218	1.254	470.112	12.527	2.539			
	3	122.259	3.117	1.157	469.115	12.495	2.513		NA	
	4	119.642	3.049	1.163	497.125	12.839	2.593			
	5	116.877	2.939	1.158	502.876	11.627	2.284			
7	1	65.706	1.787	1.078	271.560	6.292	1.969			
	2	81.718	1.531	0.822	286.725	6.845	1.868			
	3	105.414	1.595	0.742	308.381	7.518	1.889			
	4	100.211	1.451	0.719	317.376	5.966	1.637			
	5	115.202	1.432	0.696	343.568	5.853	1.574			
8	1	66.890	1.827	1.039	271.865	7.287	2.058			
	2	77.613	1.909	1.048	310.045	7.159	1.977			
	3	90.195	1.914	1.002	343.867	7.744	2.030			
	4	122.116	1.906	0.972	348.229	7.929	2.073			
	5	154.082	1.918	0.825	344.441	6.647	1.716			
9	1	**67.280**	1.764	1.043	**253.076**	6.244	1.836	**436.212**	11.325	2.654
	2	76.316	1.718	0.888	255.124	6.227	1.836	443.586	10.939	2.389
	3	95.475	1.693	0.942	272.452	5.754	1.737	464.298	11.017	2.451
	4	127.245	1.529	0.924	287.265	5.949	1.758	517.269	11.613	2.551
	5	96.895	1.847	0.976	284.899	6.240	1.619	509.753	10.066	2.306

into account, scenarios 4 to 8 were not capable of finding an acceptable solution for the problem at a heavy loading level. Still, scenario 9 remains the most successful scenario as it has the ability to improve the system performance and keep it within the specified limits. The improvement of the voltage profile obtained in scenario 9 for the system at the normal loading condition with SOPs power loss considered is shown in Fig. 10. The contribution of SOPs losses to the total power losses with different numbers of SOPs is clarified in Fig. 11, where the contour plots agree with the conclusions drawn in the IEEE 33-node case study. A detailed summary of the optimal results obtained in scenarios 5 to 9 at the normal loading condition is given in Tables A.3 and A.4 in the Appendix. Also, 83-node system is shown in Fig. 13 after applying scenario 9 at normal loading condition. Considering the main point, we conclude that the combination of NR, SOPs and DGs allocation strategies led to

Preprints (www.preprints.org) | NOT PEER-REVIEWED | Posted: 30 September 2019 doi:10.20944/preprints201909.0339.v1

Peer-reviewed version available at Energies 2019, 12, 4172; doi:10.3390/en12214172

the best solution with minimum losses and noticeably enhanced PQ indices rather than the sub-optimal solutions provided by the individual strategies, particularly at the different loading levels.

In addition, a comparison of the results obtained using the proposed algorithm and the results obtained using three conventional optimization algorithms presented in previous works [6]: genetic algorithm (GA), harmony search algorithm (HSA) and modified honeybee mating (MHM), is conducted to show the effectiveness of the DC-HSS algorithm. The proposed NR methodology is used in these optimization algorithms to find the optimal/near-optimal solutions of the NR problem for both the IEEE 33-node and 83-node distribution systems as presented in Tables 11 and 12, respectively. It can be noted that the optimal/ near-optimal (best) result is obtained using the other conventional algorithms due to usage of the proposed NR methodology but with a lower

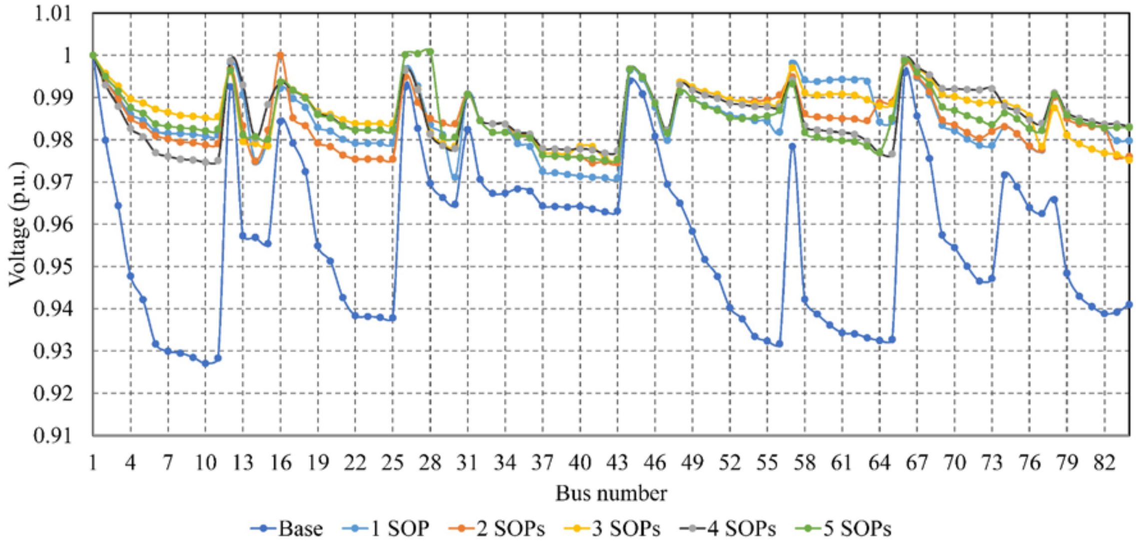

Figure 10. Improvement of the voltage profile at normal loading condition with SOPs power loss considered: scenario 9

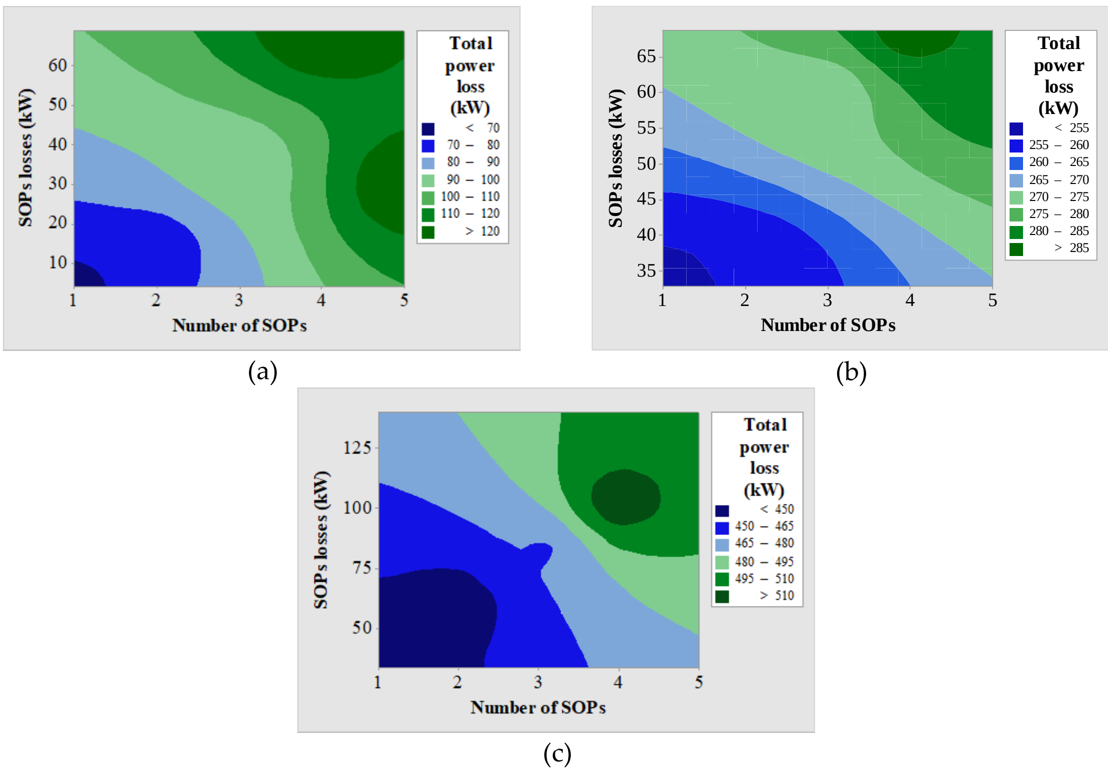

Figure 11. Contour plots of total power loss versus SOPs losses and N_{SOP}: (a) light loading, (b) normal loading, and (c) heavy loading.

Preprints (www.preprints.org) | NOT PEER-REVIEWED | Posted: 30 September 2019 doi:10.20944/preprints201909.0339.v1

Peer-reviewed version available at Energies 2019, 12, 4172; doi:10.3390/en12214172

computational time to find the best value compared to the other three algorithms, which validate the effectiveness of the proposed NR methodology regardless of the optimization technique used.

Table 11. Results obtained using the proposed and conventional optimization algorithms: IEEE 33-node distribution network

Method	DC-HSS	GA	HSA	MHM
Number of runs	30	30	30	30
Population size	2	2	2	2
Number of iterations	10	10	10	10
Best	139.55	139.55	139.55	139.55
Worst	158.4013	158.4013	158.4013	158.4013
Mean	141.6454	145.6523	151.318	149.1727
Standard deviation	5.766383	5.942117	5.231613	7.353027
Average time (s)	0.3	1	0.3	0.6

Table 12. Results obtained using the proposed and conventional optimization algorithms: 83-node distribution network

Method	DC-HSS	GA	HSA	MHM
Number of runs	30	30	30	30
Population size	2	2	2	2
Number of iterations	10	10	10	10
Best	470.241	470.241	470.241	470.241
Worst	509.7132	509.7132	509.7132	509.7132
Mean	475.5788	481.3519	506.4081	488.0029
Standard deviation	8.066826	12.24191	11.59983	12.97165
Average time (s)	0.49	2	0.5	1.7

Finally, the minimum power losses obtained by applying scenario 9 for both the IEEE 33-node and 83-node systems are presented in Table 13 compared to the power loss reported in previous works.

Table 13. Comparison of Previous Works with The Proposed Scenario 9

IEEE 33-node system				83-node system			
Ref.	Year	μ	P_{loss}^{tot} (kW)	Ref.	Year	μ	P_{loss}^{tot} (kW)
[46]	2013	NA	73.050	[43]	1996	NA	383.520
[47]	2009	NA	139.500	[44]	2005	NA	469.880
[48]	2015	NA	72.230	[45]	2014	NA	375.716
Proposed		0	**45.885**	Proposed		0	**189.073**
Proposed		1	**66.131**	Proposed		1	**253.076**

4. Conclusion

This article presents a multi-scenario analysis of optimal reconfiguration and DGs allocation in distribution networks with SOPs. The DC-HSS algorithm was used to solve the MINLP of SOPs and DGs allocation along with NR at different loading conditions to minimize the total power loss in balanced distribution systems. A new NR methodology is proposed to obtain the possible radial configurations from random configurations to minimize the power loss in two distribution systems: the IEEE 33-node and an 83-node balanced distribution system from a power company in Taiwan. Nine scenarios were investigated to find the best solution that provides the lowest power loss while improving the system performance and enhancing the PQ measures. The contribution of SOP losses to the total active losses, as well as the effect of increasing the number of SOPs connected to the system, are investigated at different loading conditions to determine the real benefits gained from their allocation. It was clear from the results obtained for scenario 9 that simultaneous NR, SOP and DG allocation into a distribution system creates a hybrid configuration that merges the benefits offered by radial distribution systems and mitigates drawbacks related to losses, PQ, and voltage violations while offering far more efficient and optimal network operation. Also, it was found that the contribution of the internal loss of SOPs to the total loss for different numbers of installed SOPs is not dependent on the number of SOPs and that loss minimization is not always guaranteed by installing more SOPs or DGs along with NR. Finally, SOPs can address issues related to voltage violations, HC, and network losses efficiently to assist the integration of DGs into distribution systems. The cost-benefit analysis was beyond the framework of the study, but it will be included in a future study using a large-scale multi-objective MINLP model of cost and benefits gained by optimal siting and sizing of SOPs and DGs in the engineering practice for large-scale balanced and unbalanced reconfigured distribution systems.

Author Contributions: Ibrahim M. Diaaeldin and Shady H.E. Abdel Aleem designed the problem under study; Ibrahim M. Diaaeldin performed the simulations and obtained the results. Shady H.E. Abdel Aleem analyzed the obtained results. Ibrahim M. Diaaeldin wrote the paper, which was further reviewed by Shady H.E. Abdel Aleem, Ahmed El-Rafei, Almoataz Y. Abdelaziz, and Ahmed F. Zobaa.

Conflicts of Interest: The authors declare no conflict of interest.

Appendix A

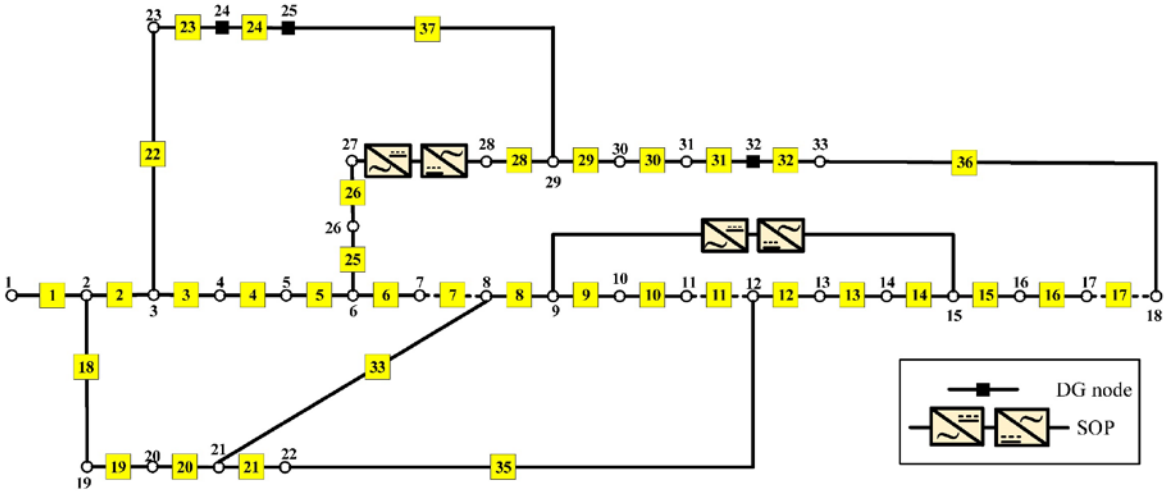

Figure 12. IEEE 33-node distribution system after NR, SOPs and DGs allocation with SOPs internal losses considered: scenario 9

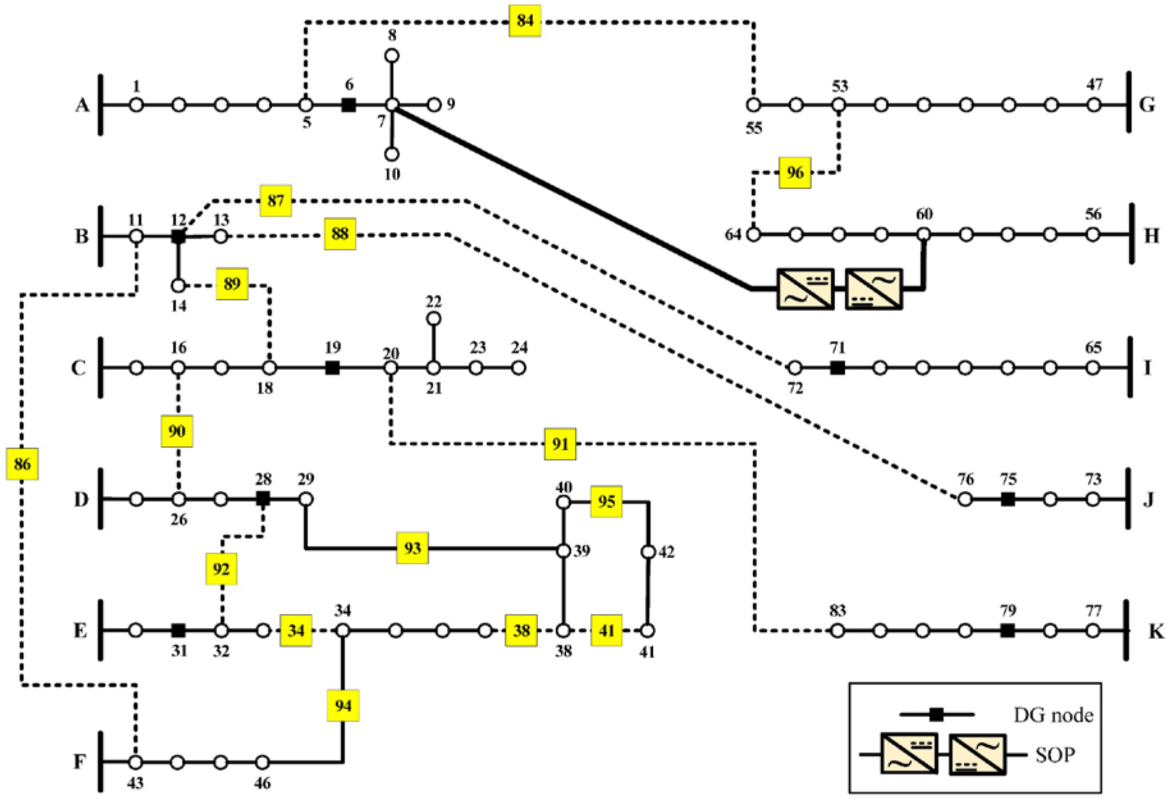

Figure 13. 83-node distribution system after NR, SOPs and DGs allocation with SOPs internal losses considered: scenario 9

Table A.1. Optimal system configuration, sizing and locations of SOPs and DGs for scenarios 4 to 9 without SOPs internal losses at normal loading level: IEEE 33-node distribution system

Scenario	tie-lines	SOPs locations (lines)	SOPs sizing			DG node	DG sizing (MW)
			P_I^{SOP} (MW)	Q_I^{SOP} (MVAr)	Q_J^{SOP} (MVAr)		
4	-	33	0.2000	0.0818	0	NA	
		34	0	0	0.0933		
		35	0.0600	0.2432	0.6847		
		36	0.0900	0.0344	0.5634		
		37	0	0	0		
5	7	11	0.0450	0.0263	0.0171	NA	
		14	-0.0600	0.2924	0.0117		
		32	-0.0600	0.3360	0.1729		
		37	-0.1200	0.2272	0.6886		
6	7	11	0.0450	0	0	NA	
		14	0	0	0.0920		
		32	-0.0600	0.3123	0.0885		
		37	-0.1200	0.3670	0.6980		
7	-	33	0	0	0.088	24	0.4200
		34	0	0	0		
		35	0.06	0	0	25	0.4200
		36	0.09	0	0	32	0.2100
		37	-0.0913	0.394984	0.521994		
8	-	7	-0.0131	0	0.173922	24	0.4200
		11	0.045	0	0		
		14	-0.06	0.071586	0	25	0.4200
		32	-0.06	0.366156	0.196486	32	0.2100
		37	-0.12	0.28405	0.521668		
9	-	7	-0.2	0.126	0.06107	24	0.4200
		11	-0.06	0	0		
		28	-0.12	0	0.812957	25	0.4200
		34	-0.06	0.036864	0.077424	32	0.2100
		36	0.09	0.286571	0.239091		

Table A.2. Optimal system configuration, sizing and locations of SOPs and DGs for scenarios 4 to 9 with SOPs internal losses considered at normal loading level: IEEE 33-node distribution system

Scenario	tie-lines	SOPs locations (lines)	SOPs sizing P_I^{SOP} (MW)	Q_I^{SOP} (MVAr)	Q_J^{SOP} (MVAr)	DG node	DG sizing (MW)
4	36	33	0.2000	0.0333	0.0538	NA	
		34	-0.0652	0.0066	0.3065		
		35	0.0600	0.1494	0.0480		
		37	-0.1252	0	0		
5	7-11-32	14	0	0	0.1582	NA	
		37	-0.1261	0.0918	0.0138		
6	7-11-32	14	-0.0628	0.0315	0.2978	NA	
		37	-0.1249	0.0009	0.8776		
7	-	33	0	0	0.082994	24	0.4200
		34	-0.06245	0	0.120284		
		35	0.06	0	0	25	0.4200
		36	0.09	0	0	32	0.2100
		37	-0.12568	0.071358	0.166987		
8	7-11-14	32	-0.0624	0	0.1901	24	0.4200
						25	0.4200
		37	-0.1260	0.0853	0.3983	32	0.2100
9	7-11-17	27	-0.0624	0.000293	0.6938	24	0.4200
						25	0.4200
		34	-0.0626	0.0243	0.2831	32	0.2100

Table A.3. Optimal system configuration, sizing and locations of SOPs and DGs for scenarios 5 to 9 without SOPs internal losses at normal loading level: 83-node distribution System

Scenario	tie-lines	SOPs locations (lines)	SOPs sizing P_I^{SOP} (MW)	SOPs sizing Q_I^{SOP} (MVAr)	SOPs sizing Q_J^{SOP} (MVAr)	DG node	DG sizing (MVA)	PF
5	13-34-39-55-63-83-86-89	7	-0.4	1.5	0.9757	NA		
		42	0.2	0.4398	0.4719			
		72	0.4184	1.4214	1.3143			
		90	0.3	0.1856	0.5016			
		92	0.7229	0.3661	1.1009			
6	13-34-39-42-84-86-89-90-96	72	1.1439	0.3959	1.4468			
		82	-0.1	1.1822	0.3869			
		85	0.4	1.4312	0.6977			
		92	-0.2	1.4781	0.6503			
7	84-86-88-89-90-91-94-95-96	85	0.1547	1.492	0.8203	6	1.100	0.9658
						12	1.200	0.9500
		87	0.2941	1.0794	0.7539	19	1.200	0.9500
						28	1.547	0.9817
		92	-0.2	0.9864	1.0761	31	1.799	0.9502
						71	2.000	0.9500
		93	0.2	0.4686	0.6413	75	1.200	0.9500
						79	2.000	0.9500
8	13-34-39-55-63-83-86-89	7	-0.4	0.5959	0.7569	6	1.100	0.9747
		42	0.200	0.4948	0.5371	12	0.995	0.9503
						19	1.200	0.9535
		72	0.3509	0.8314	0.3136	28	1.800	0.9501
						31	1.800	0.9501
		90	-0.1	1.2025	1.1796	71	1.274	0.9501
						75	1.200	0.9502
		92	-0.200	0.350	1.3027	79	2.000	0.9501
9	7-13-16-32-34-72-86-95	38	-0.02	0.239	0.493	6	1.100	0.9509
		55	0.500	1.399	0.804	12	1.200	0.9502
						19	1.200	0.9500
		64	0.300	0.9497	0.576	28	1.782	0.9500
						31	1.678	0.9501
		89	-0.091	0.764	1.236	71	2.000	0.9500
						75	1.200	0.9500
		91	0.300	0.8106	1.033	79	2.000	0.9500

 doi:10.20944/preprints201909.0339.v1

Peer-reviewed version available at *Energies* **2019**, *12*, 4172; doi:10.3390/en12214172

Table A.4. Optimal system configuration, sizing and locations of SOPs and DGs for scenarios 5 to 9 with SOPs internal losses considered at normal loading level: 83-node distribution system

Scenario	tie-lines	SOPs locations (lines)	SOPs sizing P_I^{SOP} (MW)	SOPs sizing Q_I^{SOP} (MVAr)	SOPs sizing Q_J^{SOP} (MVAr)	DG node	DG sizing (MVA)	PF
5	7-13-34-39-42-55-63-83-86-89-90-92	72	0.2605	0.4347	0.1784	NA		
6	7-13-14-34-38-40-55-63-86-90	32	-0.208	0.0098	0.5608			
		82	-0.108	0.1785	1.2975			
		87	-0.209	0.133	1.1108			
7	84-86-87-88-89-90-91-92-93-94-95-96	85	0.3367	1.4617	0.4298	6	1.100	0.9550
						12	1.200	0.9500
						19	1.200	0.9500
						28	1.800	0.9500
						31	1.800	0.9905
						71	2.000	0.9500
						75	1.200	0.9500
						79	2.000	0.9505
8	7-13-34-39-42-55-63-83-86-89-90-92	72	0.2879	0.4032	0.4376	6	1.100	0.9500
						12	1.200	0.9500
						19	1.200	0.9507
						28	1.800	0.9500
						31	1.800	0.9747
						71	2.000	0.9500
						75	1.200	0.9519
						79	2.000	0.9639
9	34-38-41-84-86-87-88-89-90-91-92-96	85	0.2091	1.3189	0.1894	6	1.100	0.9501
						12	1.200	0.9500
						19	1.200	0.9501
						28	1.800	0.9500
						31	1.800	0.9500
						71	2.000	0.9500
						75	1.200	0.9500
						79	2.000	0.9500

Preprints (www.preprints.org) | NOT PEER-REVIEWED | Posted: 30 September 2019 doi:10.20944/preprints201909.0339.v1

Peer-reviewed version available at *Energies* **2019**, *12*, 4172; doi:10.3390/en12214172

References

1. Ismael, S.; Abdel Aleem, S.; Abdelaziz, A.; Zobaa, A. Probabilistic hosting capacity enhancement in non-sinusoidal power distribution systems using a hybrid PSOGSA optimization algorithm. *Energies* **2019**, 12, 1018.
2. Home-Ortiz, J.M.; Melgar-Dominguez, O.D.; Pourakbari-Kasmaei, M.; Mantovani, J.R.S. A stochastic mixed-integer convex programming model for long-term distribution system expansion planning considering greenhouse gas emission mitigation. *Int. J. Electr. Power Energy Syst.* **2019**, *108*, 86–95.
3. Sakar, S.; Balci, M.E.; Abdel Aleem, S.H.E.; Zobaa, A.F. Integration of large- scale PV plants in non-sinusoidal environments: considerations on hosting capacity and harmonic distortion limits. *Renew. Sustain. Energy Rev*. **2018**, 82, 176–186.
4. Chicco, G.; Mazza, A. 100 years of symmetrical components. *Energies* **2019**, *12*, 450.
5. H.E. Abdel Aleem, S.; T. Elmathana, M.; F. Zobaa, A. Different design approaches of shunt passive harmonic filters based on IEEE std. 519-1992 and IEEE Std. 18-2002. *Recent Patents Electr. Electron. Eng.* **2013**, *6*, 68–75.
6. Badran, O.; Mekhilef, S.; Mokhlis, H.; Dahalan, W. Optimal reconfiguration of distribution system connected with distributed generations: A review of different methodologies. *Renew. Sustain. Energy Rev.* **2017**, *73*, 854–867.
7. Elders, I.; Ault, G.; Barnacle, M.; Galloway, S. Multi-objective transmission reinforcement planning approach for analysing future energy scenarios in the Great Britain network. *IET Gener. Transm. Distrib.* **2015**, *9*, 2060–2068.
8. Ismael, S.M.; Abdel Aleem, S.H.E.; Abdelaziz, A.Y.; Zobaa, A.F. Practical considerations for optimal conductor reinforcement and hosting capacity enhancement in radial distribution systems. *IEEE Access* **2018**, *6*, 27268–27277.
9. CHEN, S.; LIU, C.-C. From demand response to transactive energy: state of the art. *J. Mod. Power Syst. Clean Energy* **2017**, *5*, 10–19.
10. Qi, Q.; Wu, J.; Long, C. Multi-objective operation optimization of an electrical distribution network with soft open point. *Appl. Energy* **2017**, *208*, 734–744.
11. Namachivayam, G.; Sankaralingam, C.; Perumal, S.K.; Devanathan, S.T. Reconfiguration and capacitor placement of radial distribution systems by modified flower pollination algorithm. *Electr. Power Components Syst.* **2016**, *44*, 1492–1502.
12. Kazemi-Robati, E.; Sepasian, M.S. Passive harmonic filter planning considering daily load variations and distribution system reconfiguration. *Electr. Power Syst. Res.* **2019**, *166*, 125–135.
13. Schnelle, T.; Schmidt, M.; Schegner, P. Power converters in distribution grids - new alternatives for grid planning and operation. In Proceedings of the 2015 IEEE Eindhoven PowerTech; IEEE, 2015; pp. 1–6.
14. Wang, C.; Song, G.; Li, P.; Ji, H.; Zhao, J.; Wu, J. Optimal siting and sizing of soft open points in active electrical distribution networks. *Appl. Energy* **2017**, *189*, 301–309.
15. Cao, W.; Wu, J.; Jenkins, N.; Wang, C.; Green, T. Benefits analysis of soft open points for electrical distribution network operation. *Appl. Energy* **2016**, *165*, 36–47.
16. Zhang, L.; Shen, C.; Chen, Y.; Huang, S.; Tang, W. Coordinated Optimal Allocation of DGs, Capacitor Banks and SOPs in Active Distribution Network Considering Dispatching Results Through Bi-level Programming. *Energy Procedia* **2017**, *142*, 2065–2071.
17. Long, C.; Wu, J.; Thomas, L.; Jenkins, N. Optimal operation of soft open points in medium voltage electrical distribution networks with distributed generation. *Appl. Energy* **2016**, *184*, 427–437.
18. Qi, Q.; Wu, J.; Long, C. Multi-objective operation optimization of an electrical distribution network with soft open point. *Appl. Energy* **2017**, *208*, 734–744.
19. Ji, H.; Li, P.; Wang, C.; Song, G.; Zhao, J.; Su, H.; Wu, J. A strengthened SOCP-based approach for evaluating the distributed generation hosting capacity with soft open Points. *Energy Procedia* **2017**, *142*, 1947–1952.
20. Cao, W.; Wu, J.; Jenkins, N.; Wang, C.; Green, T. Operating principle of soft open points for electrical distribution network operation. *Appl. Energy* **2016**, *164*, 245–257.
21. Aithal, A.; Li, G.; Wu, J.; Yu, J. Performance of an electrical distribution network with soft open point during a grid side AC fault. *Appl. Energy* **2018**, *227*, 262–272.
22. Wang, C.; Song, G.; Li, P.; Ji, H.; Zhao, J.; Wu, J. Optimal configuration of soft open point for active distribution network based on mixed-integer second-order cone programming. *Energy Procedia* **2016**, *103*, 70–75.

Preprints (www.preprints.org) | NOT PEER-REVIEWED | Posted: 30 September 2019 doi:10.20944/preprints201909.0339.v1

Peer-reviewed version available at *Energies* **2019**, *12*, 4172; doi:10.3390/en12214172

23. Qi, Q.; Wu, J. Increasing distributed generation penetration using network reconfiguration and soft open points. *Energy Procedia* **2017**, *105*, 2169–2174.
24. Qi, Q.; Long, C.; Wu, J.; Smith, K.; Moon, A.; Yu, J. Using an MVDC link to increase DG hosting capacity of a distribution network. *Energy Procedia* **2017**, *142*, 2224–2229.
25. Li, P.; Ji, H.; Yu, H.; Zhao, J.; Wang, C.; Song, G.; Wu, J. Combined decentralized and local voltage control strategy of soft open points in active distribution networks. *Appl. Energy* **2019**, *241*, 613–624.
26. Yao, C.; Zhou, C.; Yu, J.; Xu, K.; Li, P.; Song, G. A sequential optimization method for soft open point integrated with energy storage in active distribution networks. *Energy Procedia* **2018**, *145*, 528–533.
27. Thomas, L.J.; Burchill, A.; Rogers, D.J.; Guest, M.; Jenkins, N. Assessing distribution network hosting capacity with the addition of soft open points. In Proceedings of the 5th IET International Conference on Renewable Power Generation (RPG) 2016; Institution of Engineering and Technology, 2016; pp. 1–6.
28. Guo, X.B.; Wei, W.X.; Xu, A.D. A coordinated optimization method of snop and tie switch operation simultaneously based on cost in active distribution network. In Proceedings of the IET Conference Publications; 2016.
29. Bai, L.; Jiang, T.; Li, F.; Chen, H.; Li, X. Distributed energy storage planning in soft open point based active distribution networks incorporating network reconfiguration and DG reactive power capability. *Appl. Energy* **2018**, *210*, 1082–1091.
30. Ji, H.; Wang, C.; Li, P.; Zhao, J.; Song, G.; Ding, F.; Wu, J. An enhanced SOCP-based method for feeder load balancing using the multi-terminal soft open point in active distribution networks. *Appl. Energy* **2017**, *208*, 986–995.
31. Ji, H.; Wang, C.; Li, P.; Song, G.; Wu, J. SOP-based islanding partition method of active distribution networks considering the characteristics of DG, energy storage system and load. *Energy* **2018**, *155*, 312–325.
32. Li, P.; Ji, H.; Wang, C.; Zhao, J.; Song, G.; Ding, F.; Wu, J. Coordinated control method of voltage and reactive power for active distribution networks based on soft open point. *IEEE Trans. Sustain. Energy* **2017**, *8*, 1430–1442.
33. Wang, C.; Song, G.; Li, P.; Ji, H.; Zhao, J.; Wu, J. Optimal siting and sizing of soft open points in active electrical distribution networks. *Appl. Energy* **2017**, *189*, 301–309.
34. Xiao, H.; Pei, W.; Li, K. Optimal sizing and siting of soft open point for improving the three phase unbalance of the distribution network. In Proceedings of the 2018 21st International Conference on Electrical Machines and Systems (ICEMS); IEEE, 2018; pp. 2080–2084.
35. El-Fergany, A.A. Optimal capacitor allocations using evolutionary algorithms. *IET Gener. Transm. Distrib.* **2013**, *7*, 593–601.
36. Abdelaziz, A.Y.; Ali, E.S.; Abd Elazim, S.M. Optimal sizing and locations of capacitors in radial distribution systems via flower pollination optimization algorithm and power loss index. *Eng. Sci. Technol. an Int. J.* **2016**, *19*, 610–618.
37. Karami, H.; Sanjari, M.J.; Gharehpetian, G.B. Hyper-Spherical Search (HSS) algorithm: a novel meta-heuristic algorithm to optimize nonlinear functions. *Neural Comput. Appl.* **2014**, *25*, 1455–1465.
38. Ahmadi, S.A.; Karami, H.; Sanjari, M.J.; Tarimoradi, H.; Gharehpetian, G.B. Application of hyper-spherical search algorithm for optimal coordination of overcurrent relays considering different relay characteristics. *Int. J. Electr. Power Energy Syst.* **2016**, *83*, 443–449.
39. Bloemink, J.M.; Green, T.C. Increasing photovoltaic penetration with local energy storage and soft normally-open points. In Proceedings of the 2011 IEEE Power and Energy Society General Meeting; IEEE, **2011**; pp. 1–8.
40. Bloemink, J.M.; Green, T.C. Benefits of distribution-level power electronics for supporting distributed generation growth. *IEEE Trans. Power Deliv.* **2013**, *28*, 911–919.
41. Ji, H.; Wang, C.; Li, P.; Ding, F.; Wu, J. Robust operation of soft open points in active distribution networks with high penetration of photovoltaic integration. *IEEE Trans. Sustain. Energy* **2019**, *10*, 280–289.
42. PCS 6000 for large wind turbines: Medium voltage, full power converters up to 9 MVA. ABB, brochure 3BHS351272 E01 Rev. A. **2012,** [Online]. Available: http://new.abb.com/docs/default-source/ewea-doc/pcs6000wind.pdf
43. Peponis, G.J.; Papadopulos, M.P.; Hatziargyriou, N.D. Optimal operation of distribution networks. *IEEE Trans. Power Syst.* **1996**, *11*, 59–67.
44. Chiou, J.-P.; Chang, C.-F.; Su, C.-T. Variable scaling hybrid differential evolution for solving network reconfiguration of distribution systems. *IEEE Trans. Power Syst.* **2005**, *20*, 668–674.

45. Esmaeili, S.; Dehnavi, H.D.; Karimzadeh, F. Simultaneous reconfiguration and capacitor placement with harmonic consideration using fuzzy harmony search algorithm. *Arab. J. Sci. Eng.* **2014**, *39*, 3859–3871.
46. Rao, R.S.; Ravindra, K.; Satish, K.; Narasimham, S.V.L. Power loss minimization in distribution system using network reconfiguration in the presence of distributed generation. *IEEE Trans. Power Syst.* **2013**, *28*, 317–325.
47. Abdelaziz, A.Y.; Mekhamer, S.F.; Badr, M.A.L.; Mohamed, F.M.; El-Saadany, E.F. A modified particle swarm Algorithm for distribution systems reconfiguration. In Proceedings of the 2009 IEEE Power & Energy Society General Meeting; IEEE, **2009**; pp. 1–8.
48. Rajaram, R.; Sathish Kumar, K.; Rajasekar, N. Power system reconfiguration in a radial distribution network for reducing losses and to improve voltage profile using modified plant growth simulation algorithm with Distributed Generation (DG). *Energy Reports* **2015**, *1*, 116–122.